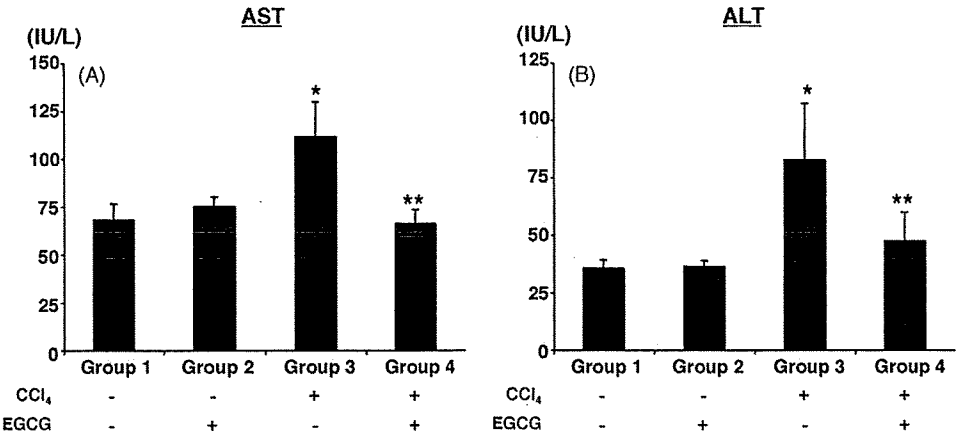

Fig. 1. Effects of EGCG on the serum levels of AST and ALT in the experimental rats. At sacrifice, blood samples were collected and the serum levels of AST (A) and ALT (B) were then assayed. Values are the means ± SE ($n = 5$). *$p < 0.01$, compared with control group (Group 1, olive oil-injected group); **$p < 0.01$, compared with CCl_4-injected group (Group 3).

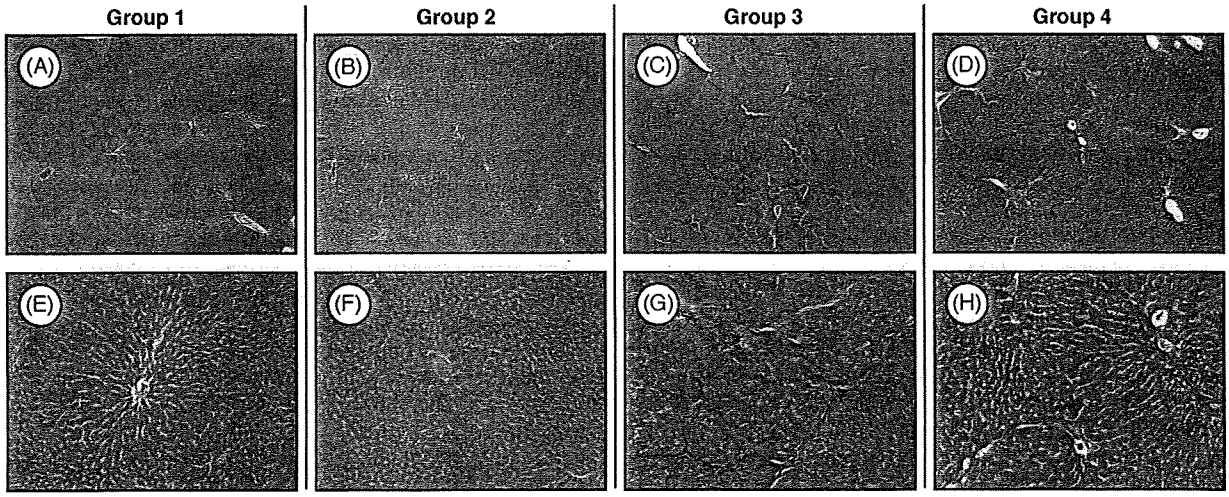

Fig. 2. Photomicrographs of liver sections from the rats in control group (Group 1, A and E), olive oil-injected and EGCG drinking group (Group 2, B and F), CCl_4-injected group (Group 3, C and G) and CCl_4-injected and EGCG drinking group (Group 4, D and H). Paraffin-embedded sections were stained with Azan stain to show fibrosis. Original magnification: ×40 (A–D) and ×100 (E–H).

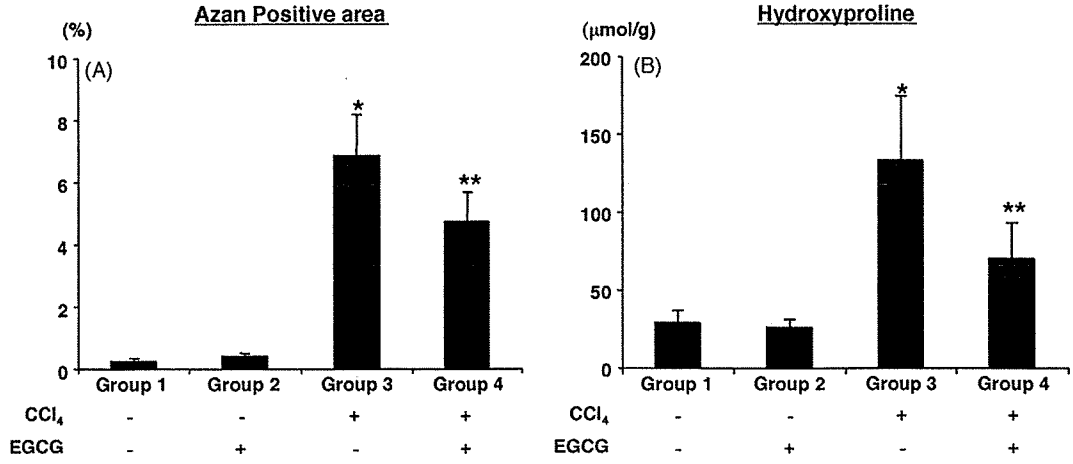

Fig. 3. Effects of EGCG on hepatic fibrosis area and hydroxyproline content in the experimental rats. (A) The fibrosis area was evaluated by Azan stain (Fig. 2) using an image analyzer. (B) The hepatic hydroxyproline contents were quantified colorimetrically, as described in Section 2. Values are the means ± SE ($n = 5$). *$p < 0.01$, compared with control group (Group 1); **$p < 0.01$, compared with CCl_4-injected group (Group 3).

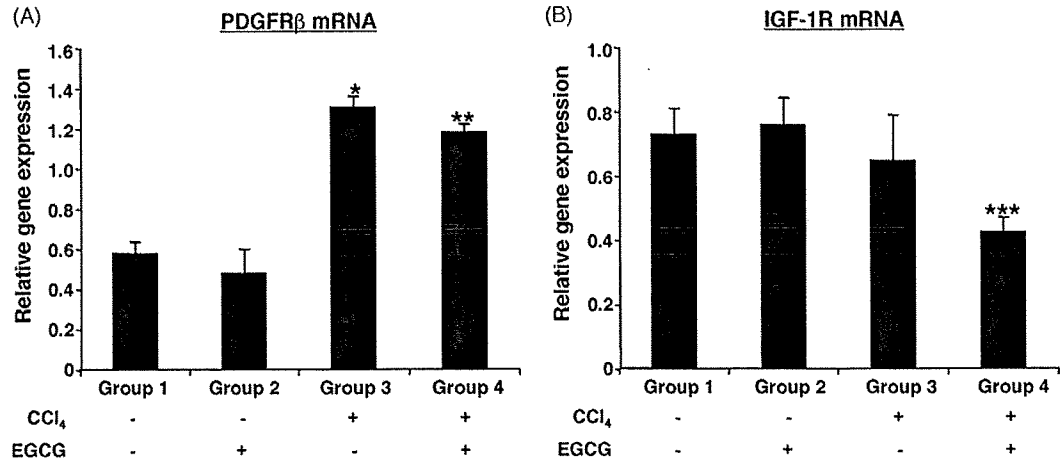

Fig. 4. Effects of EGCG on the expression levels of PDGFRβ and IGF-1R mRNAs in the experimental rats. cDNA was synthesized from the livers of experimental rats and real-time PCR was performed using PDGFRβ (A) and IGF-1R (B) specific primers. The expression levels of these genes were normalized to the level of *GAPDH* gene. Values are the means ± SE ($n = 5$). *$p < 0.01$, compared with control group (Group 1); **$p < 0.05$, compared with CCl_4-injected group (Group 3); ***$p < 0.01$, compared with CCl_4-injected group (Group 3).

in the olive oil-injected group either with (Fig. 2B and F) or without EGCG (Fig. 2A and E). A densitometric analysis showed the fibrosis areas to be markedly suppressed in the EGCG-treated rats (Fig. 3A, $p < 0.01$). Similar findings were also observed in measurements of the liver hydroxyproline contents; in the CCl_4-injected rats, drinking water with 0.1% EGCG caused a significant decrease in the amounts of hydroxyproline observed in the liver (Fig. 3B).

3.3. Effects of EGCG on the expression of PDGFRβ and IGF-1R mRNAs in the liver of the CCl_4-injected rats

To elucidate the possible mechanisms in regard to how EGCG attenuates liver fibrosis (Figs. 2 and 3), the effects of this agent on the expression levels of PDGFRβ and IGF-1R mRNAs in the experimental liver were then examined because these RTKs play a critical role in the development of liver fibrosis [1,5,13]. The expression level of PDGFRβ mRNA was elevated in the liver of CCl_4-injected rats and drinking EGCG significantly lowered the level of this mRNA raised by CCl_4 (Fig. 4A). No significant increase was observed in the level of IGF-1R mRNA by CCl_4 injection, whereas treatment with EGCG remarkably decreased the expression of this mRNA (Fig. 4B).

3.4. Effects of EGCG on the expression of PDGFRβ and α-SMA proteins in the liver of the CCl_4-injected rats

Next, the effects of EGCG on the expression levels of PDGFRβ and α-SMA, an indicator of HSC activation, in the rat liver were examined using a Western blot analysis. As shown in Fig. 5A, the intraperitoneal injection of CCl_4 markedly increased the levels of both PDGFRβ and α-SMA proteins in the experimental rat liver. On the other hand, drinking EGCG significantly decreased the expression of PDGFRβ as well as α-SMA proteins raised by CCl_4 (Fig. 5A). Immunohistochemical analysis also indicated that the α-SMA-immunoreactive areas remarkably increased in the liver of the CCl_4-injected group when compared to the olive oil-injected group. In addition, drinking EGCG significantly reduced the expression area of this protein, thus indicating the inhibition of HSC activation (Fig. 5B).

4. Discussion

The activation of HSCs, which is induced by PDGF/PDGFR interaction, plays a pivotal role in the development of liver fibrosis [1,5]. Therefore, targeting the PDGF/PDGFR axis is considered to be an effective strategy to inhibit the progress of hepatic fibrosis. Yoshiji et al. [14] reported that, imatinib mesylate, a clinically used PDGFR tyrosine kinase inhibitor, markedly attenuated liver fibrosis in rats by inhibiting the PDGF-induced proliferation and migration of activated HSCs. The present study demonstrates that drinking EGCG significantly suppressed the liver injury caused by CCl_4 (Fig. 1). Moreover, the results of the present study clearly indicate that EGCG effectively prevented the development of liver fibrosis (Figs. 2 and 3) and this finding was associated with the inhibition of the expression of PDGFRβ and α-SMA (Figs. 4A and 5). These findings are consistent with those of a previous *in vitro* report which showed EGCG to inhibit both HSC proliferation and *PDGFRβ* gene expression by blocking the activation of AP-1 and NF-κB [20]. This report seems to be interesting because these transcription factors are regarded as effective targets of EGCG to exert its anticancer properties [9,21].

Several studies have pointed the interactions between the IGF-1R and PDGF/PDGFR axis in the development of liver fibrosis. For instance, PDGF stimulated the IGF-1R mRNA expression through the activation of the *IGF-1R* gene promoter [22]. Functional IGF-1R was required for the mitogenic activity of the PDGFR in liver myofibroblasts [13]. The cooperative activation of the intracellular signaling pathways, including extracellular signal-regulated kinase (ERK) and Akt, by PDGF and IGF-1 played an important role in perpetuating the activated state of HSC during liver fibrogenesis [23]. Recent studies have revealed that EGCG in drinking water suppressed obesity-related colonic carcinogenesis by inhibiting the activation of the IGF/IGF-1R axis in the colonic mucosa [10]. Treatment of HepG2 human HCC cells with EGCG also decreased the production of IGF-1 from these cancer cells, thus inhibiting the phosphorylation of IGF-1R and its downstream ERK and Akt proteins [11]. These reports, together with our present finding that drinking EGCG significantly reduced the expression of IGF-1R mRNA in the fibrotic liver (Fig. 4B), may suggest that EGCG, which targets both the PDGF/PDGFR and IGF/IGF-1R axes, might also be useful for inhibiting liver fibrosis.

Moreover, in addition to the effects of EGCG on specific RTKs, recent studies have indicated that green tea polyphenols may also possess other anti-fibrotic properties, such as antioxidant properties. EGCG has also been shown to arrest the progression of hepatic fibrosis in the rat model by inhibiting oxidative damage [24]. Supplementation with green tea extract inhibited a progression of cirrhosis in a rat model of steatohepatitis and this was associated with its antioxidant and radical scavenging activities [25]. These

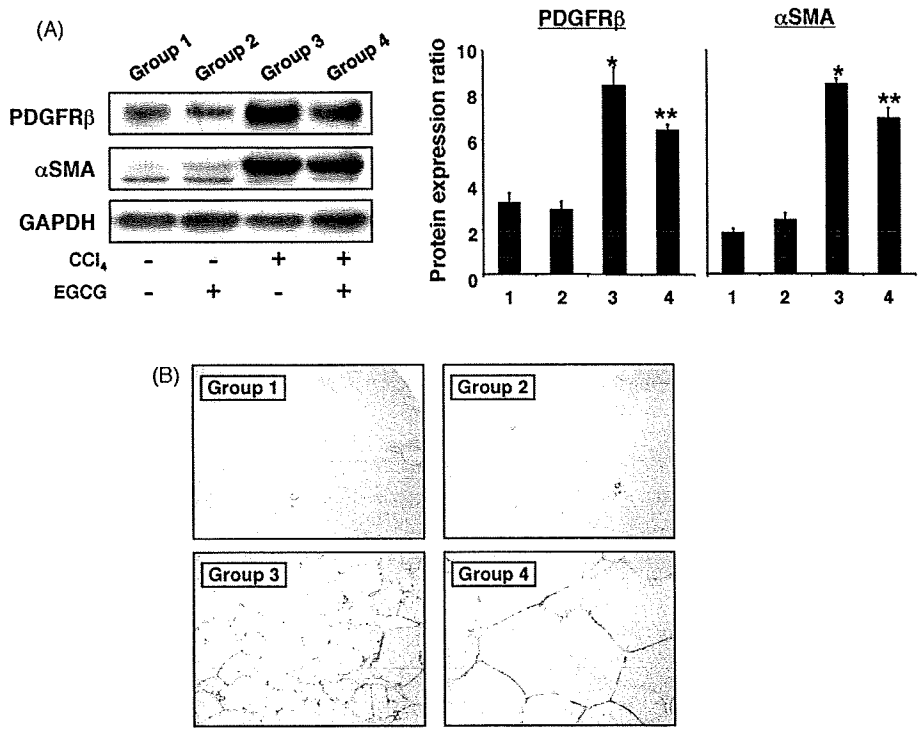

Fig. 5. Effects of EGCG on the expression levels of PDGFRβ and α-SMA in the experimental rats. (A) Total protein was extracted from the liver of experimental rats and equivalent amounts of protein were examined by a Western blot analysis using the respective antibodies. An antibody to GAPDH served as a loading control. Repeat Western blots gave similar results. The results obtained from Western blot analysis were quantitated by densitometry and are displayed in the right panels. Values are the means ± SE ($n=5$). $^{*}p<0.01$, compared with control group (Group 1); $^{**}p<0.01$, compared with CCl_4-injected group (Group 3). (B) Immunohistochemical expression of α-SMA in the liver of control group (Group 1), olive oil-injected and EGCG drinking group (Group 2), CCl_4-injected group (Group 3) and CCl_4-injected and EGCG drinking group (Group 4). Original magnification: ×40.

reports also support the possibility that the administration of EGCG is useful for preventing the progression of hepatic fibrosis. In conclusion, the ability of EGCG to target PDGFR and IGF-1R, both of which play critical roles in the progression of liver fibrosis, is considered to provide evidence that this naturally occurring agent may be effective in both the prevention and therapy of liver fibrosis.

Conflict of interest

The authors declare no conflicts of interest.

Acknowledgments

We thank Drs. Naoto Ishibashi and Tetsuro Sano at Kowa Pharmaceutical Co., Ltd (Tokyo, Japan) for their support and encouragement.

References

[1] S.L. Friedman, Mechanisms of hepatic fibrogenesis, Gastroenterology 134 (2008) 1655–1669.
[2] G. Fattovich, T. Stroffolini, I. Zagni, F. Donato, Hepatocellular carcinoma in cirrhosis: incidence and risk factors, Gastroenterology 127 (2004) S35–S50.
[3] H. Yoshida, R. Tateishi, Y. Arakawa, M. Sata, S. Fujiyama, S. Nishiguchi, H. Ishibashi, G. Yamada, O. Yokosuka, Y. Shiratori, M. Omata, Benefit of interferon therapy in hepatocellular carcinoma prevention for individual patients with chronic hepatitis C, Gut 53 (2004) 425–430.
[4] Y. Shiratori, F. Imazeki, M. Moriyama, M. Yano, Y. Arakawa, O. Yokosuka, T. Kuroki, S. Nishiguchi, M. Sata, G. Yamada, S. Fujiyama, H. Yoshida, M. Omata, Histologic improvement of fibrosis in patients with hepatitis C who have sustained response to interferon therapy, Ann. Intern. Med. 132 (2000) 517–524.
[5] E. Borkham-Kamphorst, C.R. van Roeyen, T. Ostendorf, J. Floege, A.M. Gressner, R. Weiskirchen, Pro-fibrogenic potential of PDGF-D in liver fibrosis, J. Hepatol. 46 (2007) 1064–1074.
[6] L. Wong, G. Yamasaki, R.J. Johnson, S.L. Friedman, Induction of beta-platelet-derived growth factor receptor in rat hepatic lipocytes during cellular activation in vivo and in culture, J. Clin. Invest. 94 (1994) 1563–1569.
[7] M. Pinzani, S. Milani, H. Herbst, R. DeFranco, C. Grappone, A. Gentilini, A. Caligiuri, G. Pellegrini, D.V. Ngo, R.G. Romanelli, P. Gentilini, Expression of platelet-derived growth factor and its receptors in normal human liver and during active hepatic fibrogenesis, Am. J. Pathol. 148 (1996) 785–800.
[8] C.S. Yang, P. Maliakal, X. Meng, Inhibition of carcinogenesis by tea, Annu. Rev. Pharmacol. Toxicol. 42 (2002) 25–54.
[9] M. Shimizu, A. Deguchi, J.T. Lim, H. Moriwaki, L. Kopelovich, I.B. Weinstein, (−)-Epigallocatechin gallate and polyphenon E inhibit growth and activation of the epidermal growth factor receptor and human epidermal growth factor receptor-2 signaling pathways in human colon cancer cells, Clin. Cancer Res. 11 (2005) 2735–2746.
[10] M. Shimizu, Y. Shirakami, H. Sakai, S. Adachi, K. Hata, Y. Hirose, H. Tsurumi, T. Tanaka, H. Moriwaki, (−)-Epigallocatechin gallate suppresses azoxymethane-induced colonic premalignant lesions in male C57BL/KsJ-db/db mice, Cancer Prev. Res. 1 (2008) 298–304.
[11] M. Shimizu, Y. Shirakami, H. Sakai, H. Tatebe, T. Nakagawa, Y. Hara, I.B. Weinstein, H. Moriwaki, EGCG inhibits activation of the insulin-like growth factor (IGF)/IGF-1 receptor axis in human hepatocellular carcinoma cells, Cancer Lett. 262 (2008) 10–18.
[12] A. Sachinidis, C. Seul, S. Seewald, H. Ahn, Y. Ko, H. Vetter, Green tea compounds inhibit tyrosine phosphorylation of PDGF beta-receptor and transformation of A172 human glioblastoma, FEBS Lett. 471 (2000) 51–55.
[13] R. Novosyadlyy, J. Dudas, R. Pannem, G. Ramadori, J.G. Scharf, Crosstalk between PDGF and IGF-I receptors in rat liver myofibroblasts: implication for liver fibrogenesis, Lab. Invest. 86 (2006) 710–723.
[14] H. Yoshiji, R. Noguchi, S. Kuriyama, Y. Ikenaka, J. Yoshii, K. Yanase, T. Namisaki, M. Kitade, T. Masaki, H. Fukui, Imatinib mesylate (STI-571) attenuates liver fibrosis development in rats, Am. J. Physiol. Gastrointest. Liver Physiol. 288 (2005) G907–G913.
[15] T. Ogiso, M. Nagaki, S. Takai, Y. Tsukada, T. Mukai, K. Kimura, H. Moriwaki, Granulocyte colony-stimulating factor impairs liver regeneration in mice through the up-regulation of interleukin-1beta, J. Hepatol. 47 (2007) 816–825.
[16] M. Shimizu, A. Hara, M. Okuno, H. Matsuno, K. Okada, S. Ueshima, O. Matsuo, M. Niwa, K. Akita, Y. Yamada, N. Yoshimi, T. Uematsu, S. Kojima, S.L. Friedman, H. Moriwaki, H. Mori, Mechanism of retarded liver regeneration in plasminogen activator-deficient mice: impaired activation of hepatocyte growth factor after Fas-mediated massive hepatic apoptosis, Hepatology 33 (2001) 569–576.
[17] H. Tomita, Y. Yamada, T. Oyama, K. Hata, Y. Hirose, A. Hara, T. Kunisada, Y. Sugiyama, Y. Adachi, H. Linhart, H. Mori, Development of gastric tumors in Apc(Min/+) mice by the activation of the beta-catenin/Tcf signaling pathway, Cancer Res. 67 (2007) 4079–4087.

[18] N. Kociok, S. Radetzky, T.U. Krohne, C. Gavranic, A.M. Joussen, Pathological but not physiological retinal neovascularization is altered in TNF-Rp55-receptor-deficient mice, Invest. Ophthalmol. Vis. Sci. 47 (2006) 5057–5065.
[19] T. Saito, S. Akutsu, T. Urushiyama, K. Ishibashi, Y. Nakagawa, C.F. Shuler, A. Yamane, Changes in the mRNA expressions of insulin-like growth factors, their receptors, and binding proteins during the postnatal development of rat masseter muscle, Zoolog. Sci. 20 (2003) 441–447.
[20] A. Chen, L. Zhang, The antioxidant (−)-epigallocatechin-3-gallate inhibits rat hepatic stellate cell proliferation in vitro by blocking the tyrosine phosphorylation and reducing the gene expression of platelet-derived growth factor-beta receptor, J. Biol. Chem. 278 (2003) 23381–23389.
[21] M. Shimizu, A. Deguchi, A.K. Joe, J.F. McKoy, H. Moriwaki, I.B. Weinstein, EGCG inhibits activation of HER3 and expression of cyclooxygenase-2 in human colon cancer cells, J. Exp. Ther. Oncol. 5 (2005) 69–78.
[22] M. Rubini, H. Werner, E. Gandini, C.T. Roberts Jr., D. LeRoith, R. Baserga, Platelet-derived growth factor increases the activity of the promoter of the insulin-like growth factor-1 (IGF-1) receptor gene, Exp. Cell Res. 211 (1994) 374–379.
[23] K.R. Bridle, L. Li, R. O'Neill, R.S. Britton, B.R. Bacon, Coordinate activation of intracellular signaling pathways by insulin-like growth factor-1 and platelet-derived growth factor in rat hepatic stellate cells, J. Lab. Clin. Med. 147 (2006) 234–241.
[24] M.C. Zhen, Q. Wang, X.H. Huang, L.Q. Cao, X.L. Chen, K. Sun, Y.J. Liu, W. Li, L.J. Zhang, Green tea polyphenol epigallocatechin-3-gallate inhibits oxidative damage and preventive effects on carbon tetrachloride-induced hepatic fibrosis, J. Nutr. Biochem. 18 (2007) 795–805.
[25] K. Nakamoto, F. Takayama, M. Mankura, Y. Hidaka, T. Egashira, T. Ogino, H. Kawasaki, A. Mori, Beneficial effects of fermented green tea extract in a rat model of non-alcoholic steatohepatitis, J. Clin. Biochem. Nutr. 44 (2009) 239–246.

Biochemical and Biophysical Research Communications 381 (2009) 733–737

Contents lists available at ScienceDirect

Biochemical and Biophysical Research Communications

journal homepage: www.elsevier.com/locate/ybbrc

Extracellular matrix is required for the survival and differentiation of transplanted hepatic progenitor cells

Yoshihiko Tsukada, Masahito Nagaki *, Atsushi Suetsugu, Yosuke Osawa, Hisataka Moriwaki

Department of Gastroenterology, Gifu University Graduate School of Medicine, 1-1 Yanagido, Gifu 501-1194, Japan

ARTICLE INFO

Article history:
Received 24 February 2009
Available online 4 March 2009

Keywords:
EHS gel
Extracellular matrix
Differentiation
Stem cell
Hepatocyte
Transplantation

ABSTRACT

Engelbreth–Holm–Swarm (EHS) gel has been reported to maintain the mature hepatocyte phenotypes in primary cultured hepatocytes. We investigated the effect of EHS gel on the differentiation of fetal liver cells, which contain stem/progenitor cells. The isolated fetal liver cells cultured on EHS gel formed a spherical shape and increased liver-specific gene expressions compared with cells cultured on collagen. The hepatic progenitor cells that were transplanted subcutaneously to BALB/c nude mice could survive and express hepatocyte marker alpha-fetoprotein when the cells were suspended with EHS gel. These findings demonstrate that EHS gel supports cytodifferentiation from immature progenitor cells to hepatocytes and maintain its differentiated phenotypes *in vitro* and *in vivo*.

Extracellular matrix (ECM) plays an important role in cell survival, proliferation, and differentiation [1]. Adhesive interactions between hepatocyte and ECM retain its differentiated phenotypes and maintain liver-specific functions, accompanied with up-regulation of the liver-enriched transcription factors including hepatocyte nuclear factor (HNF)s [2,3]. Lamining-rich ECM, Engelbreth–Holm–Swarm sarcoma (EHS) gel has been reported to keep a high expression of liver-specific products such as albumin, and normal cell polarity and structure for prolonged periods in primary cultured hepatocytes [4]. On the other hand, culture on dried type 1 collagen leads the cells to dedifferentiated phenotypes such as flattened monolayer and low expression of liver-specific proteins [2,5].

Liver transplantation is the primary treatment for severe liver diseases. However, the therapy is limited because of insufficient organ availability, and cell transplantation is believed to become alternative therapy. Various types of cells are reported as candidates for cell transplantation for liver diseases. THLE-5b cells, an immortalized non-tumorigenic human cell line, were well localized in the peritoneal cavity of BALB/c nude mice for 3 weeks after cell transplantation [6]. Immortalized human hepatocytes provide life saving metabolic supports in rats when they are transplanted into spleen [7].

Recently, stem cells have been thought to be suitable source of cell transplantation for liver diseases. Bone marrow derived mesenchymal stem cells rescued experimental mouse liver failure when they were engrafted to the liver [8]. Human embryonic stem cells [9], oval cells [10], and cord blood cells [11] are also reported to have the potential to develop into viable hepatocytes. However, these cells might be too immature to be directed to mature differentiated hepatocytes. Fetal liver cells contain stem/progenitor cells, which are able to differentiate bipotentially into hepatocytes and cholangiocytes, and represent differentiated property of hepatocyte by transduction of HNF-4 gene [12] or culture on ECM [13]. However, it is still not known if the cells cultured on EHS gel survive and function as the mature hepatocytes. In this study, we investigated if the hepatic stem/progenitor cells obtain and retain the differentiated hepatocyte phenotypes under such condition *in vitro* and *in vivo*.

Materials and methods

Fetal liver cell isolation and culture. The beta-actin promoter-driven GFP-transgenic mice (GFP mice) were bred for studies. Pregnant female C57BL/6J mice were purchased from Nippon SLC (Sizuoka, Japan). Fetal mouse liver parenchymal cells were harvested as previously reported [12]. Briefly, the cells were isolated from the embryonic day 14.5 livers by mechanical pipetting. Hematopoietic cells were removed by magnetically activated cell sorter using a Lineage cell depletion kit (Miltenyi Biotec, Bergisch Gladbach, Germany). Then the separated fetal liver cells were plated on either normal plastic, EHS gel coated (BD Bioscience,

Abbreviations: EHS gel, Engelbreth–Holm–Swarm gel; AFP, alpha-fetoprotein; ECM, extracellular matrix; HNF, hepatocyte nuclear factor; GFP, green fluorescent protein; CK-19, cytokeratin-19; GAPDH, glyceraldehyde 3-phosphate dehydrogenase; C/EBP, CCAAT/enhancer binding protein.

* Corresponding author. Fax: +81 58 230 6310.
E-mail address: mnagaki@gifu-u.ac.jp (M. Nagaki).

0006-291X/$ - see front matter © 2009 Elsevier Inc. All rights reserved.
doi:10.1016/j.bbrc.2009.02.158

Bedford, MA, USA), or type 1 collagen coated dishes (Iwaki, Tokyo, Japan) (5×10^6 cells/100 mm dish) in DMEM/F12 medium (Gibco BRL, Gaithersburg, MD, USA) supplemented with 10^{-6} M insulin (Wako, Osaka, Japan), 10^{-7} M dexamethasone (Wako), 10% fetal bovine serum (ThermoTrace, Melbourne, Australia), 10 mM nicotinamide (Wako), 50 μM β-mercaptoethanol (Sigma Chemical Co., St. Louis, MO, USA), 5 mM HEPES (Wako), and 100 U/ml penicillin and 100 μg/ml streptomycin (Gibco). The medium was replaced every other day. Animal use and experimentation was performed under the strict guidelines of the Institutional Animal Use and Care Committee at the Gifu University Graduate School of Medicine.

Immunohistochemistry. The cells were fixed by methanol at −20 °C for 10 min, and washed in PBS including 0.05% polyoxyethylene sorbitan monolaurate (Tween 20) (Wako). Nonspecific binding was blocked with 10% nonimmune rabbit serum. Fixed cells were incubated with the rabbit primary antibodies, fluorescein isothiocyanate-conjugated anti-mouse albumin (BETHYL, Montgomery, TX, USA) and anti-mouse cytokeratin 19 (CK19, gift from Dr. N. Tanimizu, Kanagawa Academy of Science and Technology, Japan), in a moist chamber at 4 °C for 16 h. After washing in PBS-Tween 20, cells were incubated with Texas Red-conjugated goat anti-rabbit IgG (Invitrogen, CA, USA) at 4 °C for 3 h to detect CK19. Nuclear counterstain was performed with 4′,6-diamidino-2-phenylindole. The signal was detected using a fluorescence microscope (Olympus, Tokyo, Japan).

Quantitative real-time RT-PCR. Fetal liver cells were cultured for 4 days and detached by cell scraper. Total RNA was isolated from the cells using ISOGEN (Wako). For each sample, 2.0 μg of total RNA was reverse-transcribed using a high-capacity complementary DNA reverse transcription kit as described by the manufacturer (Applied Biosystems, Foster City, CA, USA). The mRNA quantification was performed using a 2-step real-time RT-PCR (Light Cycler, Roche Diagnostics, IN, USA) with Light cycler TaqMan Master and Universal ProbeLibrary Probes (Roche). The PCR primers and probes were as follows; albumin (sense, 5′-CCAAAGT CAACAAGGAGTGCT-3′; antisense 5′-TCGCCTGGTTTTCACACAT-3′; probe #62), HNF-4 (sense, 5′-CCGAGGGACGATGTAGTCAT-3′; antisense 5′-CAAGAGGTCCATGGTGTTCA-3′; probe #68), CK19 (sense, 5′-CCTCAGGGCAGTAATTTCCTC-3′; antisense 5′-TGACCTGGAGATG CAGATTG-3′; probe #17). Target complementary DNAs were normalized to the endogenous mRNA levels of 18S ribosomal RNA (sense, 5′-GCTCTTAGAATTACCACAGTTATCC-3′; antisense, 5′-AATCAGTTATGGTTCCTTTGTCG-3′; probe #55).

Western blot analysis. For the preparation of total cell proteins, the cells cultured for 4 days on the dishes were homogenized in the radioimmunoprecipitation lysis buffer (Santa Cruz, CA, USA). The protein concentration was measured using a DC-protein assay (Bio-Rad). The extracted proteins (10 μg) were separated by SDS–PAGE and then transferred onto a nitrocellulose membrane (Bio-Rad). The membranes were first incubated with the primary antibodies against albumin (Santa Cruz, sc-46293), HNF-4 (Santa Cruz, sc-6556), HNF-1 (Santa Cruz, sc-8986), CK19 (Santa Cruz, sc-33119), alpha-fetoprotein (AFP) (Santa Cruz, sc-8108) and glyceraldehyde 3-phosphate dehydrogenase (GAPDH) (Cell Signaling, #2118) and then incubated with the HRP-coupled secondary antibodies (Santa Cruz). Detection was performed using ECL system (Amersham Biosciences, NJ, USA).

Cell transplantation to nude mice. To determine the effect of EHS gel on cell survival and cytodifferentiation *in vivo*, the fetal liver cells (1×10^5 cells) isolated from GFP mice were suspended in EHS gel, collagen gel (0.3% Cellmatrix type 1-A, Nitta-Gelatin), or DMEM/F12 medium, and then injected subcutaneously to 6-week-old male BALB/c nude mice (Nippon SLC). The grafts were removed with skin tissue at 3 weeks after transplantation, and observed with fluorescent microscope to detect GFP. The sections were stained with hematoxylin and eosin (HE). Immunohistochemical staining for AFP were performed with anti-AFP antibody (Santa Cruz, sc-8108) using avidin–biotin–peroxidase complex technique (Vector, Burlingame, CA, USA).

Results

Morphology and hepatic gene expression of fetal liver cells on different culture substrate

We have previously shown that the fetal liver contains hepatic stem/progenitor cells [12]. When the fetal liver cells were cultured on EHS gel coated dishes, cells formed clusters like a spherical shape 4 days after inoculation. In contrast, the cells showed a flattened and extended shape on type 1 collagen coated or normal plastic dish (Fig. 1). The spherical cells on EHS gel and flattened, extended cells on collagen or plastic dishes expressed albumin, a hepatocyte marker, and CK19, a cholangiocyte marker. In cells on collagen and plastic, cells located in the center of colonies were stained by albumin antibody, whereas the peripheral cells were mainly stained by CK19 antibody. These results indicate that fetal liver cells have bipotent differentiation ability.

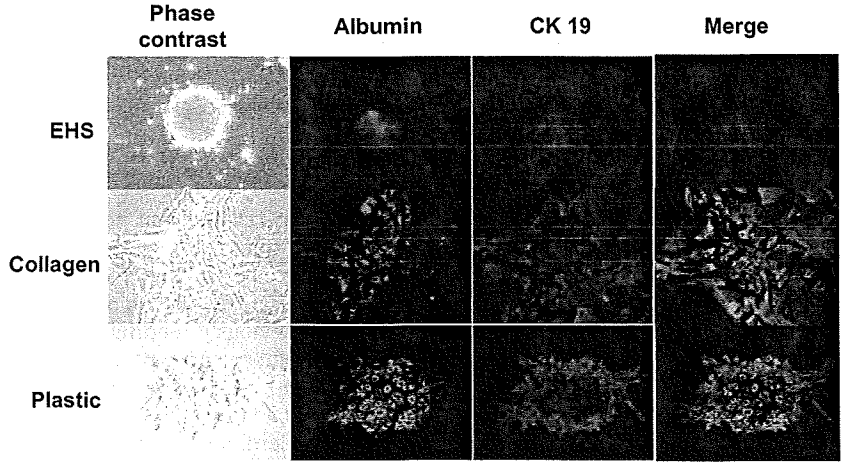

Fig. 1. Morphological changes of the fetal liver cells cultured on ECMs. The isolated fetal liver cells were cultured on each indicated ECMs for 4 days. Expression of albumin (green) and CK19 (red) were examined by double immunofluorescent staining with anti-albumin and CK 19 antibodies. The fluorescence was visualized with fluorescent conforcal microscope. (Original magnification ×200.)

Effects of ECMs on the liver-specific genes and proteins

As observed in immunohistochemistry, Western blot analysis also showed that the protein level of albumin was higher in the cells cultured on EHS gel than in the cells on type 1 collagen or plastic dish 4 days after culture. Reversely, CK19 was higher in the cells on type 1 collagen or plastic dish (Fig. 2A). Another hepatocyte maker AFP was also higher in the cells on EHS gel (A). Moreover, HNF-4 and -1 proteins were also higher in the cells on EHS gel. In parallel with the protein expressions, mRNA of albumin was higher in the cells cultured on EHS gel and CK19 mRNA was higher in the cells on type 1 collagen (Fig. 2B). These results demonstrate that EHS gel supports cytodifferentiation of hepatic stem/progenitor cells to hepatocytes.

Cell transplantation to nude mice

On the basis of these findings, we performed a further experiment to examine the cytodifferentiation ability of EHS gel *in vivo*. The fetal liver cells were isolated from GFP mice, were suspended with EHS gel, collagen gel, or DMEM medium, and were transplanted into subcutaneous tissues of BALB/c nude mice. The

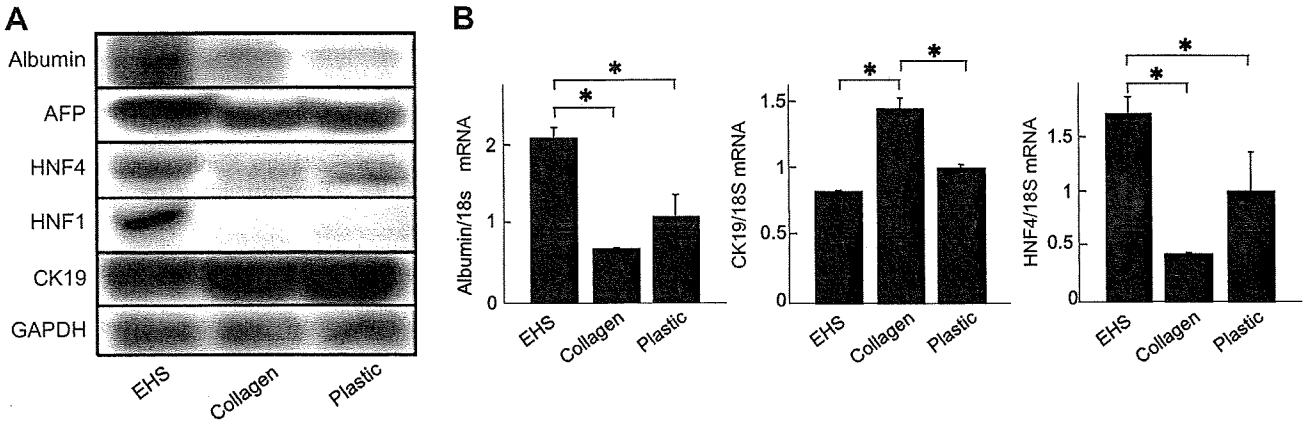

Fig. 2. Liver-specific protein and gene expressions of the fetal liver cells cultured on ECMs. The isolated fetal liver cells were cultured on each indicated ECMs for 4 days. (A) Extracted proteins were subjected to SDS–PAGE, and immunoblotting was performed with anti-albumin, AFP, HNF-4, HNF-1, CK19, and GAPDH antibodies. (B) mRNA levels of albumin, CK19, and HNF-4 in the cultured cells were determined by quantitative real-time RT-PCR. Data are means ± SD from at least three independent experiments. *, $P < 0.05$ using Student's *t*-test.

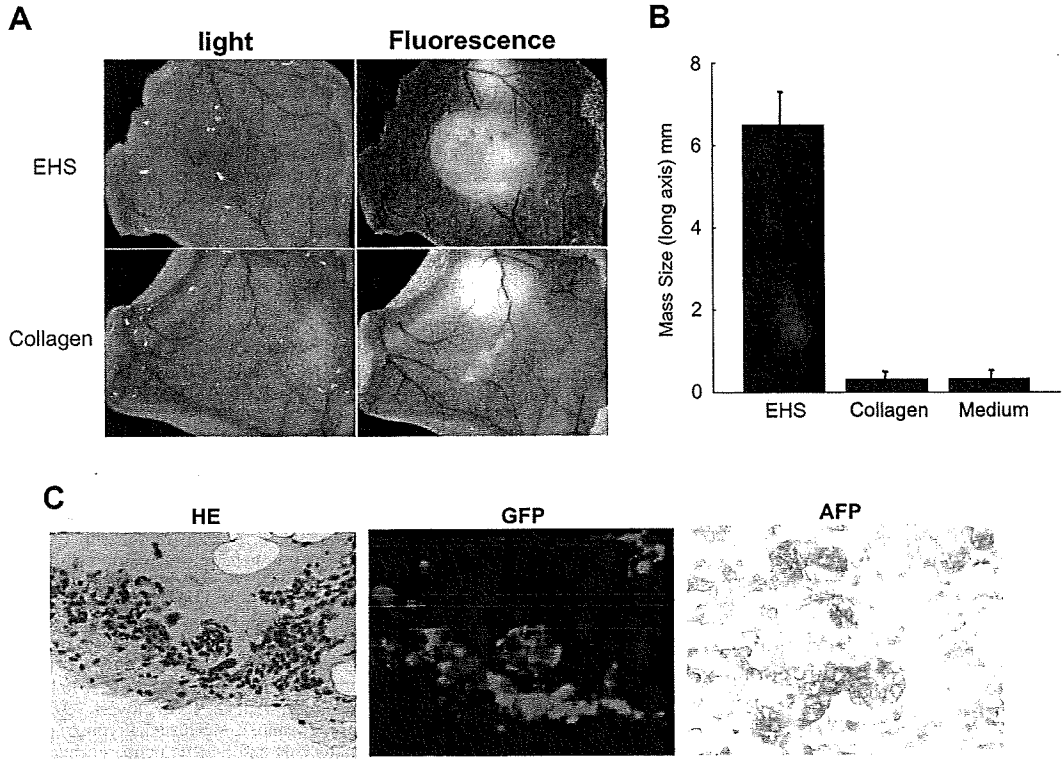

Fig. 3. Transplantation of the fetal liver cells with ECMs into BALB/c nude mice. (A) The fetal liver cells were isolated from GFP mice. The cells were suspended with EHS gel, collagen gel, or DMEM medium, and then transplanted subcutaneously into BALB/c nude mice. The animals were killed at 3 weeks after transplantation, and subcutaneous tissue was excised and photographed with light (left panels) or fluorescence (right panels). (B) The mass size (long axis) of the GFP positive area was measured. Data are means ± SD from at least three independent experiments. (C) The grafts of fetal liver cells with EHS gel were excised and stained with HE (left panel). GFP fluorescence was detected with fluorescence confocal microscope (middle panel). Expression of AFP was examined 12 days after transplantation by immunohistochemistry with anti-AFP antibody (right panel). (Original magnification ×200.)

grafted fetal liver cells with EHS gel remained even 3 weeks after transplantation, whereas cells with collagen gel or DMEM medium showed faint GFP signals (Fig. 3A and B). Moreover, the transplanted cells with EHS gel expressed AFP (Fig. 3C). These results suggest that EHS gel is able to maintain the cell survival and supports cytodifferentiation to hepatocyte *in vivo*.

Discussion

Cell transplantation has been investigated for an alternative therapy of liver organ transplantation. Differentiated hepatoma cell lines or primary cultured hepatocytes from adult liver have been thought as potential candidates [9]. However, hepatoma cells provide low levels of liver functions, and primary cultured hepatocytes rapidly lose their differentiated phenotypes and show a reduction of liver-specific gene expression once they are plated on plastic dishes [14]. Several ECMs are reported to maintain differentiated hepatocyte phenotypes. EHS gel modulates the shapes of cultured rat hepatocytes [14] and rat small hepatocytes [15]. EHS gel keeps hepatocyte-phenotypic gene expression through high expression of liver-enriched transcription factors, such as HNF-4 [16], and enhances many liver-specific functions [17]. EHS gel or sandwich culture with collagen gel maintains features of mature hepatocytes such as albumin expression, and they are attempted to use for development of bioartificial liver system [3]. However, insufficient availability of donor organ is still a problem because primary cultured hepatocytes have less regenerative ability. Thus, it would be greatly beneficial for cell transplantation if functional hepatocytes could be generated from other sources. Recently, stem cells, which have abilities of self-renewal and multilineage differentiation, are highlighted as candidates for cell transplantation. Liver stem cells can be isolated from the fetal liver, and these cells have extensive replication ability and maintain the expression of liver-specific genes, such as albumin and CK19, for prolonged cultured period [12].

In this study, we demonstrated that EHS gel promoted cytodifferentiation of hepatic progenitor cells to hepatocytes and maintained their efficiency as hepatocytes consistent with primary cultured adult hepatocytes. Interaction with ECM influenced the cell morphology and maturation of fetal liver cells. In matured hepatocytes, cells in spheroids retain the *in vivo* levels of albumin and glucokinase, whereas cells in monolayer lose the differentiated phenotypes [18]. Organization of the cytoskeleton by cell–cell and cell–ECM interaction associates with liver-specific gene expression [19]. Indeed, actin depolymerization in hepatocytes by EHS gel increases HNF-4 and albumin expression [20]. In small hepatocytes, morphological changes of the cells induce specific liver-enriched transcription factors such as HNF-4α, HNF-6, C/EBPα, and C/EBPβ [21]. HNF-4 is a key molecule for fetal liver development [22]. Overexpression of HNF-4 in hepatic progenitor cells increases liver-specific gene expression such as albumin and ApoA1 [12]. Reversely, blockage of HNF-4 expression by siRNA inhibits the up-regulation of the liver-specific gene expression in primary cultured hepatocytes cultured on EHS gel [20]. These findings and our results indicate that EHS gel induces the morphological change of hepatic progenitor cells to a spherical shape, and that HNF-4 expression via the organization of the cytoskeleton might be required for the cytodifferentiation of hepatic progenitor cells.

The differentiation potential of fetal liver cells to hepatocytes was also supported by EHS gel *in vivo*. The fetal liver cells suspended with EHS gels kept their viability and AFP expression, suggesting that cell–ECM interaction is also required for cell survival and cytodifferentiation to the hepatocyte *in vivo*. Hepatocyte transplantation into liver has been performed via portal vain for various liver diseases [23,24]. The transplanted cells might interact with ECM of the liver. Consistent with our results, it has been reported that ECM components are the predominant factor to maintain hepatocytes at heterotopic sites [25]. Ectopic subcutaneous hepatocyte transplantation may have advantages as follows; (i) surgical operation is not required, (ii) risk of embolisms is low, and (iii) the transplanted cells are removable or replaceable. Of note, the ectopic cells require additional ECMs such as EHS gel to maintain hepatocyte functions.

In conclusions, our results indicate that EHS gel promotes the differentiation of hepatic progenitor cells to functional hepatocytes. We also demonstrated that EHS gel supports cytodifferentiation and maintains the cell survival and functions *in vivo*. Our findings may therefore have relevance to the clinical application of ectopic liver stem/progenitor cell transplantation as an option to treat liver diseases.

Acknowledgements

We are grateful to Prof. Takahiro Kunisada (Gifu University Graduate School of Medicine) for providing the GFP-transgenic mice.

References

[1] J.A. McDonald, Matrix regulation of cell shape and gene expression, Curr. Opin. Cell Biol. 1 (1989) 995–999.
[2] M. Nagaki, Y. Shidoji, Y. Yamada, A. Sugiyama, M. Tanaka, T. Akaike, H. Ohnishi, H. Moriwaki, Y. Muto, Regulation of hepatic genes and liver transcription factors in rat hepatocytes by extracellular matrix, Biochem. Biophys. Res. Commun. 210 (1995) 38–43.
[3] M. Nagaki, K. Miki, Y.I. Kim, H. Ishiyama, I. Hirahara, H. Takahashi, A. Sugiyama, Y. Muto, H. Moriwaki, Development and characterization of a hybrid bioartificial liver using primary hepatocytes entrapped in a basement membrane matrix, Dig. Dis. Sci. 46 (2001) 1046–1056.
[4] E.G. Schuetz, D. Li, C.J. Omiecinski, U. Muller-Eberhard, H.K. Kleinman, B. Elswick, P.S. Guzelian, Regulation of gene expression in adult rat hepatocytes cultured on a basement membrane matrix, J. Cell. Physiol. 134 (1988) 309–323.
[5] J.P. Iredale, M.J. Arthur, Hepatocyte-matrix interactions, Gut 35 (1994) 729–732.
[6] T. Tokiwa, T. Yamazaki, W. Xin, N. Sugae, M. Noguchi, S. Enosawa, T. Tsukiyama, Differentiation potential of an immortalized non-tumorigenic human liver epithelial cell line as liver progenitor cells, Cell Biol. Int. 30 (2006) 992–998.
[7] N. Kobayashi, T. Fujiwara, Karen A. Westerman, Y. Inoue, Prevention of acute liver failure in rats with reversibly immortalized human hepatocytes, Science 287 (2000) 1258–1262.
[8] Tom K. Kuo, Shun-Pei Hung, Chiao-Hui Chuang, Chien-Tsun Chen, Yu-Ru V. Shih, Szu-Ching Y. Fang, Vincent W. Yang, Oscar K. Lee, Stem cell therapy for liver disease: parameters governing the success of using bone marrow mesenchymal stem cells, Gastroenterology 134 (2008) 2111–2121.
[9] Y. Duan, A. Catana, Y. Meng, N. Yamamoto, S. He, S. Gupta, S.S. Gambhir, M.A. Zern, Differentiation and enrichment of hepatocyte-like cells from human embryonic stem cells in vitro and in vivo, Stem Cells 25 (2007) 3058–3068.
[10] S. Gupt, D.R. LaBrecque, D.A. Shafritz, Mitogenic effects of hepatic stimulator substance on cultured nonparenchymal liver epithelial cells, Hepatology 15 (1992) 485–491.
[11] P.N. Newsome, I. Johannessen, S. Boyle, E. Dalakas, K.A. Mcaulay, K. Samuel, F. Rae, L. Forrester, M.L. Turner, P.C. Hayes, D.J. Harrison, W.A. Bickmore, J.N. Plevris, Human cord blood-derived cells can differentiate into hepatocytes in the mouse liver with no evidence of cellular fusion, Gastroenterology 124 (2003) 1891–1900.
[12] A. Suetsugu, M. Nagaki, H. Aoki, T. Motohashi, T. Kunisada, H. Moriwaki, Differentiation of mouse hepatic progenitor cells induced by hepatocyte nuclear factor-4 and cell transplantation in mice with liver fibrosis, Transplantation 86 (2008) 1178–1186.
[13] A. Kamiya, N. Kojima, T. Kinoshita, Y. Sakai, A. Miyaijma, Maturation of fetal hepatocytes *in vitro* by extracellular matrices and oncostatin M: induction of tryptophan oxygenase, Hepatology 35 (2002) 1351–1359.
[14] D.M. Bissell, D.M. Anderson, J.J. Maher, F.J. Roll, Support of cultured hepatocytes by a laminin-rich gel, J. Clin. Invest. 79 (1987) 801–812.
[15] T. Mitaka, F. Sato, T. Yokono, Y. Mochizuki, Reconstruction of hepatic organoid by rat small hepatocytes and hepatic nonparenchymal cells, Hepatology 29 (1999) 111–125.
[16] H. Oda, K. Nozawa, Y. Hitomi, A. Kakinuma, Laminin-rich extracellular matrix maintains high level of hepatocyte nuclear factor 4 in rat hepatocyte culture, Biochem. Biophys. Res. Commun. 212 (1995) 800–805.
[17] E.G. Schuets, D. Li, C.J. Omiecinski, U. Muller-Eberhard, H.K. Kleinman, B. Elswick, P.S. Guzelian, Regulation of gene expression in adult rat hepatocytes cultured on a basement membrane matrix, J. Cell. Physiol. 134 (1988) 309–323.

[18] C. Yuasa, Y. Tomita, K. Ishimura, A. Ichihara, Importance of cell aggregation for expression of liver functions and regeneration demonstrated with primary cultured hepatocytes, J. Cell. Physiol. 156 (1993) 522–530.
[19] A. Ben-Ze'ev, G.S. Robinson, N.L. Bucher, S.R. Farmer, Cell–cell and cell–matrix interactions differentially regulate the expression of hepatic and cytoskeletal genes in primary cultures of rat hepatocytes, Proc. Natl. Acad. Sci. USA 85 (1988) 2161–2165.
[20] T. Kimata, M. Nagaki, Y. Tsukada, T. Ogiso, H. Moriwaki, Hepatocyte nuclear factor-4 alpha and -1 small interfering RNA inhibits hepatocyte differentiation induced by extracellular matrix, Hepatol. Res. 35 (2006) 3–9.
[21] S. Sugimoto, T. Mitaka, S. Ikeda, K. Harada, I. Ikai, Y. Yamaoka, Y. Mochizuki, Morphological changes induced by extracellular matrix are correlated with maturation of rat small hepatocytes, J. Cell. Biochem. 87 (2002) 16–28.
[22] F.M. Sladek, W.M. Zhong, E. Lai, J.E. Darnell, Liver-enriched transcription factor HNF-4 is a novel member of the steroid hormone receptor superfamily, Genes Dev. 4 (1990) 2353–2365.
[23] M. Muraca, G. Gerunda, D. Neri, M.T. Vilei, A. Granato, P. Feltracco, M. Meroni, G. Giron, A.B. Burlina, Hepatocyte transplantation as a treatment for glycogen storage disease type 1a, Lancet 359 (2002) 317–318.
[24] A. Dhawan, R.R. Mitry, R.D. Hughes, S. Lehec, C. Terry, S. Bansal, R. Arya, J.J. Wade, A. Verma, N.D. Heaton, M. Rela, G. Mieli-Vergani, Hepatocyte transplantation for inherited factor VII deficiency, Transplantation 78 (2004) 1812–1814.
[25] K. Ohashi, M.A. Kay, H. Kuge, T. Yokoyama, H. Kanehiro, M. Hisanaga, S. Ko, M. Nagao, M. Sho, Y. Nakajima, Heterotopically transplanted hepatocyte survival depends on extracellular matrix components, Transplant. Proc. 37 (2005) 4587–4588.

Biochemical and Biophysical Research Communications 389 (2009) 229–234

Contents lists available at ScienceDirect

Biochemical and Biophysical Research Communications

journal homepage: www.elsevier.com/locate/ybbrc

Interaction between LPS-induced NO production and IDO activity in mouse peritoneal cells in the presence of activated Vα14 NKT cells

Hirofumi Ohtaki [a], Hiroyasu Ito [a,*], Kazuki Ando [a], Tetsuya Ishikawa [c], Masato Hoshi [a], Ryo Tanaka [a], Yosuke Osawa [a], Takashi Yokochi [e], Hisataka Moriwaki [b], Kuniaki Saito [d], Mitsuru Seishima [a]

[a] Department of Informative Clinical Medicine, Gifu University Graduate School of Medicine, 1-1 Yanagido, Gifu 501-1194, Japan
[b] First Department of Internal Medicine, Gifu University Graduate School of Medicine, 1-1 Yanagido, Gifu 501-1194, Japan
[c] Cancer Immunotherapy Center, Nagoya Kyoritsu Hospital, 1-195 Hoge, Nakagawa, Nagoya, Aichi 454-0933, Japan
[d] Human Health Sciences, Graduate School of Medicine and Faculty of Medicine, Kyoto University, 53 Kawahara-cho, Shogoin, Sakyo, Kyoto 606-8507, Japan
[e] Department of Microbiology and Immunology, Aichi Medical University, Nagakute, Aichi 480-1195, Japan

ARTICLE INFO

Article history:
Received 19 August 2009
Available online 26 August 2009

Keywords:
Nitric oxide
Indoleamine 2,3-dioxygenase
Peritoneal cells
Vα14 NKT cell
Lipopolysaccharide
α-Galactosylceramide

ABSTRACT

In this study, we demonstrated that lipopolysaccharide (LPS) markedly increased nitric oxide (NO) production and indoleamine 2,3-dioxygenase (IDO) activity in mouse peritoneal cells in the presence of activated Vα14 natural killer T cells. Moreover, LPS-induced NO production in peritoneal cells from IDO-knockout (KO) mice was more increased than that from wild-type mice. However, there was no significant difference in the expression of inducible nitric oxide synthase (iNOS) mRNA and protein between the wild-type and IDO-KO mice. No significant difference was also observed in the ratio of CD3- and DX5-positive cells and F4/80- and TLR4-positive cells in peritoneal cells between the wild-type and IDO-KO mice. Since the IDO activity was enhanced by an NO inhibitor, NO may be post-translationally consumed by inhibiting the IDO activity. IDO is well known to play an important role in immunosuppression during inflammatory disease. Therefore, the inhibition of IDO by NO may exacerbate inflammation in the peritoneal cavity.

Introduction

Vα14 natural killer T (NKT) cells produce large amounts of both Th1 and Th2 cytokines on stimulation with the ligand, α-galactosylceramide (α-GalCer), and they play a crucial role in various immune responses [1,2]. In particular, interferon (IFN)-γ is known to promote macrophage activation and enhance inducible nitric oxide synthase (iNOS) expression [3]. Bacterial infection strongly induces iNOS, and considerable nitric oxide (NO) is produced to attack bacteria [4]. On the other hand, NO is also known to cause severe cell and tissue injury [5–8]. Previously, we reported that NO production by α-GalCer-treated peritoneal cells and intra-hepatic lymphocytes was highly sensitive to lipopolysaccharide (LPS) stimulation [9,10]. These findings suggest that even mild LPS stimulation is dangerous in the presence of activated NKT cells.

Indoleamine 2,3-dioxygenase (IDO) catalyzes the rate-limiting step in the kynurenine pathway of tryptophan degradation [11]. In many cell types, IDO is strongly induced by IFN-γ and tumor necrosis factor (TNF)-α during an inflammatory response. IDO plays a important role in the suppression of acute inflammatory responses and regulates both innate and acquired immunity [12,13]. IDO and some downstream metabolites also contribute to the generation of regulatory T (Treg) cells, which are involved in immunotolerance and anti-inflammation [14–16]. Thus, IDO maintains the immune balance in inflammatory diseases by curbing the response.

Recently, experiments have shown that IDO is inhibited by NO and peroxynitrite, a reactant in the reaction between NO and superoxide [17,18]. However, few studies have addressed the significance of this interaction between NO and IDO in the acute inflammatory model under conditions of excessive NO production. Gram-negative bacterial infection with primary disease involving NKT cells activation is predicted that both LPS and IFN-γ derived from activated NKT cells increase NO production and IDO activity in macrophages. Peritoneal cells are well known to have a large proportion of macrophages, which may contribute to acute inflammation after bacterial infection. If we find that NKT cells activated by α-GalCer enhance both LPS-induced NO production and IDO activity in peritoneal cells, it may provide a clue to understanding the interaction between NO and IDO in the peritoneal cavity under inflammatory conditions in the presence of activated NKT cells. Therefore, the aim of our study was to investigate the effect of α-GalCer-activated NKT cells on LPS-induced NO production and IDO activity and the subsequent interaction between NO and IDO.

* Corresponding author. Fax: +81 58 230 6431.
E-mail address: hito@gifu-u.ac.jp (H. Ito).

0006-291X/$ - see front matter © 2009 Elsevier Inc. All rights reserved.
doi:10.1016/j.bbrc.2009.08.120

Materials and methods

Reagents. Synthesized α-GalCer was provided by Kirin Brewery Company (Gunma, Japan). LPS from *Escherichia coli* O55:B5 and Nω-nitro-L-arginine methyl ester hydrochloride (L-NAME) were purchased from Sigma Chemical Co. (St. Louis, MO, USA).

Mice. C57BL/6 mice at approximately 8 weeks of age were obtained from Japan SLC (Hamamatsu, Japan). IDO-knockout (KO) mice were obtained from Jackson Laboratory (Bar Harbor, ME, USA). All animal procedures were conducted in accordance with the National Institutes of Health Guide for the Care and Use of Laboratory Animals, and the guidelines for care and use of animals established by the Animal Care and Use Committee of Gifu University.

Cell preparation and culture. The mice were sacrificed at 0 h (non-treatment) and 12 h (α-GalCer-treatment) after intravenous administration of α-GalCer (1 μg/mouse). Peritoneal cells were obtained and suspended in RPMI 1640 medium (Wako Pure Chemical Industries, Osaka, Japan) containing 10% heat-inactivated fetal bovine serum (Thermo Fisher Scientific, Inc., Waltham, MA, USA) and cultured at 37 °C in a 5% CO_2 atmosphere.

Determination of nitrite concentration. Peritoneal cells from wild-type and IDO-KO mice were cultured with LPS (1–100 ng/mL) for 24 h. The nitrite concentration of the culture medium was estimated by the Griess reaction [19]. The culture medium (100 μL) was mixed with 100 μL of Griess reagent, and incubated at room temperature for 10 min, after which the absorbance was measured at 570 nm by using a microplate reader.

Assay of IDO activity. IDO activity was assessed using the methylene blue/ascorbate assay as described previously [20]. Briefly, the cell lysate was centrifuged at 7000*g* at 4 °C for 10 min. The supernatant (50 μL) was reacted with the substrate solution (50 μL) at 37 °C for 60 min. The substrate solution comprised 100 mM potassium phosphate buffer (pH 6.5), 50 μM methylene blue, 20 μg catalase, 50 mM ascorbate, and 0.4 mM L-tryptophan. After incubation, the samples were acidified with 3% perchloric acid and centrifuged at 7000*g* at 4 °C for 10 min. The concentration of L-kynurenine (L-KYN) was measured by high-performance liquid chromatography (HPLC). IDO activity was expressed as the L-KYN content per hour per milligram protein.

Real-time PCR analysis. Real-time reverse transcription polymerase chain reaction (RT-PCR) was used to quantify the levels of iNOS, IDO, IFN-γ, and TNF-α mRNA. Total RNA was isolated using an RNeasy mini kit (Qiagen GmbH, Hilden, Germany) and transcribed to cDNA by using the High capacity cDNA transcription kit (Applied Biosystems, Foster City, CA, USA). Purified cDNA was used as the template for real-time PCR conducted using pre-designed primer/probe sets for iNOS, IDO, IFN-γ, TNF-α, and 18S rRNA (Applied Biosystems), according to the manufacturer's recommendations. 18S rRNA was used as an internal control. Real-time PCR was carried out using a Light-Cycler Rapid Thermal Cycler System (Roche Diagnostic Systems, Indianapolis, IN, USA).

Western blot analysis. Peritoneal cells from α-GalCer-treated wild-type and IDO-KO mice were cultured with LPS (10 ng/mL) for 24 h. Protein (20 μg) from the cell lysate was subjected to sodium dodecyl sulfate–polyacrylamide gel electrophoresis (SDS–PAGE) and transferred to a nitrocellulose membrane. The membrane was blocked with 5% skim milk, and incubated with anti-NOS2, anti-IDO, and anti-GAPDH antibodies for 60 min at room temperature and subsequently incubated with peroxidase-labeled anti-mouse or anti-rabbit IgG for 60 min at room temperature. Immunoreactive protein bands were visualized with ECL plus (GE Healthcare UK Ltd., England).

Flow cytometric analysis. Flow cytometry was used to evaluate the phenotype of the peritoneal cells at 0 and 12 h after α-GalCer-treatment. Following reaction with anti-CD16/CD32 antibody to suppress non-specific binding, the peritoneal cells were stained with fluorescein-isothiocyanate (FITC)-conjugated anti-F4/80 antibody, phycoerythrin (PE)-conjugated anti-Toll-like receptor 4 (TLR4) antibody, FITC-conjugated anti-CD3 antibody, and PE-conjugated anti-DX5 antibody. The peritoneal cells were phenotypically characterized using FACScan (Becton–Dickinson, San Jose, CA, USA). CD3- and DX5-positive cells were considered as NKT cells, and F4/80- and TLR4-positive cells were considered as macrophages.

Statistical analysis. In each experiment, the results were expressed as means ± SD. The statistical significance of the difference in mean values was determined by Student's *t*-test or one-way analysis of variance followed by Scheffe's test. *P* values of less than 0.05 were considered significant.

Results

Effect of α-GalCer on LPS-induced NO production and IDO activity in peritoneal cells from wild-type and IDO-KO mice

To examine the effect of α-GalCer-pre-treatment on LPS-induced NO production, peritoneal cells (at a rate of 1×10^5 cells/well) from non-treated and α-GalCer-treated wild-type mice were cultured with 100 ng/mL LPS for 24 h. LPS-induced NO production was greater in peritoneal cells from α-GalCer-treated mice than in those from non-treated mice. In particular, the peritoneal cells obtained from the mice at 12 h after α-GalCer-treatment exhibited significantly greater LPS-induced NO production than those obtained after 6 and 48 h after α-GalCer-treatment (Fig. 1A), which was in keeping with the results of a previous report [8]. Therefore, peritoneal cells from the mice at 12 h after α-GalCer-treatment were used for the following experiments unless stated otherwise.

LPS-induced IDO activity was examined in peritoneal cells from wild-type and IDO-KO mice treated with or without α-GalCer. Peritoneal cells (at a rate of 3×10^6 cells/well) were cultured with 100 ng/mL LPS for 24 h. The LPS-induced IDO activity of the peritoneal cells from the α-GalCer-treated mice was markedly greater than that of cells from non-treated mice. On the other hand, IDO activity was not observed in the peritoneal cells from the IDO-KO mice (Fig. 1B).

Since previous reports suggested that NO interacts with IDO [17,18], we examined the effect of α-GalCer on LPS-induced NO production in wild-type and IDO-KO mice. Peritoneal cells from wild-type and IDO-KO mice treated with or without α-GalCer were cultured at a rate of 1×10^5 cells/well with LPS (1, 10, and 100 ng/mL) for 24 h. The extent of LPS-induced NO production was almost equal between the peritoneal cells from non-treated wild-type mice and IDO-KO mice (Fig. 1C). On the other hand, LPS-induced NO production was much greater in the peritoneal cells from α-GalCer-treated IDO-KO mice than in those from α-GalCer-treated wild-type mice (Fig. 1D).

LPS-induced mRNA and protein expression of iNOS and IDO in peritoneal cells from α-GalCer-treated wild-type and IDO-KO mice

As the second step in our experiment, we examined the expression of iNOS and IDO mRNA and protein in peritoneal cells from α-GalCer-treated wild-type and IDO-KO mice. The expression of iNOS and IDO mRNA in peritoneal cells stimulated with LPS (10 ng/mL) for 12 h was analyzed by real-time RT-PCR and was determined on the basis of 18S rRNA expression. No significant difference was observed in the expression of iNOS mRNA between the α-GalCer-treated wild-type and IDO-KO mice (Fig. 2A). The expression of IDO mRNA in the peritoneal cells from wild-type mice was significantly enhanced by LPS stimulation (Fig. 2B). The protein level

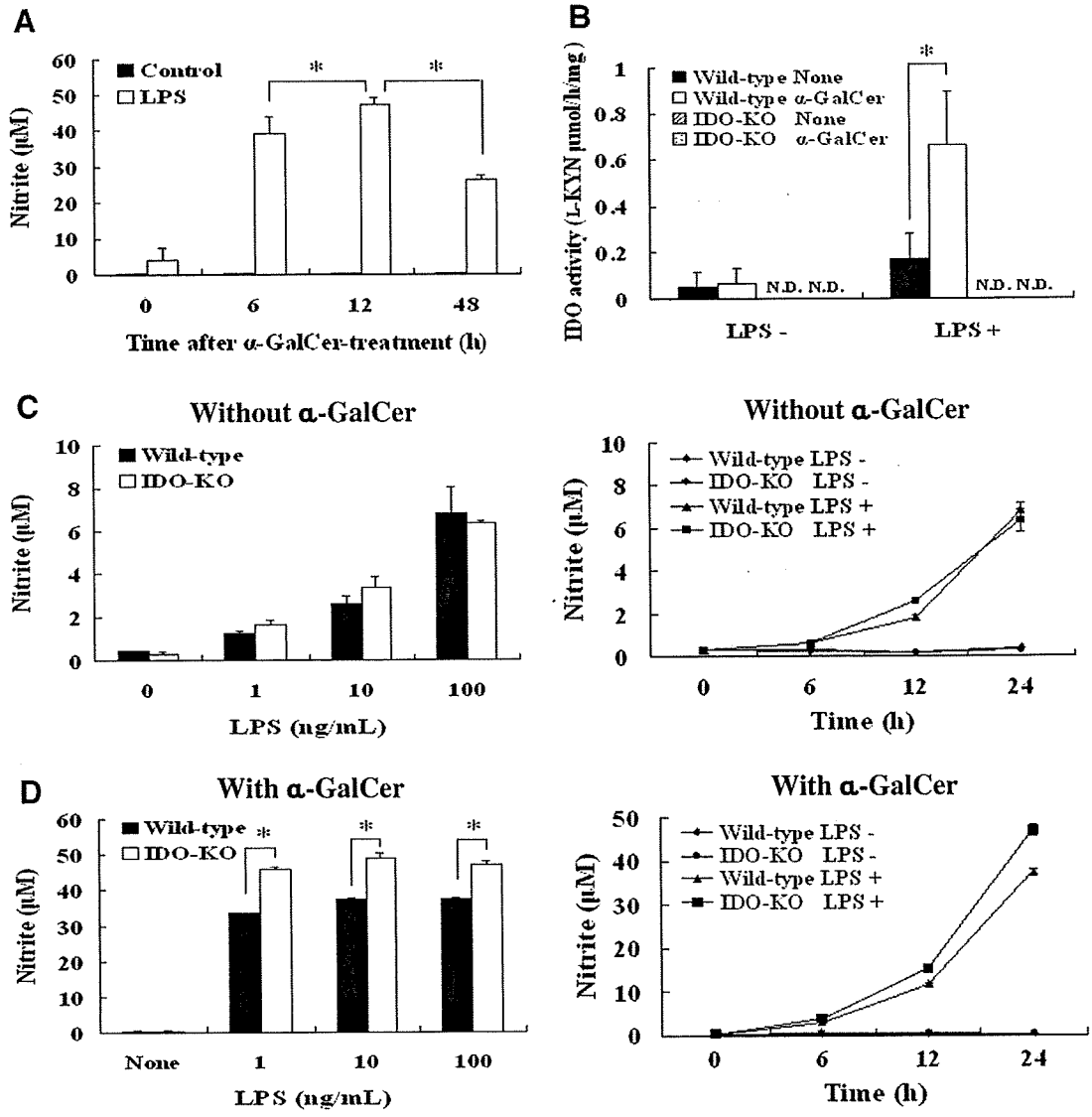

Fig. 1. Effect of α-GalCer on LPS-induced NO production and IDO activity in peritoneal cells. Peritoneal cells from the mice obtained at 0, 6, 12, and 48 h after α-GalCer-treatment were cultured at a rate of 1×10^5 cells/well with LPS (100 ng/mL), and the concentration of nitrite in the culture medium was determined (A). Peritoneal cells from non-treated and α-GalCer-treated wild-type and IDO-KO mice were cultured at a rate of 3×10^6 cells/well with LPS (100 ng/mL) for 24 h, and the IDO activity of the cell lysate was determined (B). Peritoneal cells from non-treated (C) and α-GalCer-treated (D) wild-type and IDO-KO mice were cultured at a rate of 1×10^5 cells/well with LPS (1, 10, and 100 ng/mL) for 24 h. In the time-course analysis of NO production, LPS was used at a concentration of 100 ng/mL. The data are represented as means ± SD of the results of three samples from each group. *$P < 0.05$; N.D.: not detected.

of iNOS and IDO in the peritoneal cells stimulated with LPS (10 ng/mL) for 24 h was examined by Western blot analysis and was determined on the basis of GAPDH protein expression. NO difference in the iNOS protein expression was observed between the α-GalCer-treated wild-type and IDO-KO mice. Further, in the wild-type mice, IDO protein was only expressed in the presence of LPS (Fig. 2C).

Effects of α-GalCer on IFN-γ and TNF-α expression and on the phenotype of peritoneal cells from wild-type and IDO-KO mice

Since Vα14 NKT cells activated by α-GalCer rapidly produce IFN-γ and TNF-α, which are closely related to iNOS expression, IFN-γ and TNF-α mRNA in peritoneal cells was analyzed at 0, 3, and 12 h after α-GalCer-treatment by using real-time PCR. There was no significant difference in the expression of IFN-γ and TNF-α mRNA between the wild-type and IDO-KO mice (Fig. 3A and B). Further, we examined the percentage of NKT cells (DX5- and CD3-positive cells) and macrophages (F4/80- and TLR4-positive cells) among the peritoneal cells from wild-type and IDO-KO mice by flow cytometry. No significant difference was observed in the ratio of CD3- and DX5-positive cells between the wild-type and IDO-KO mice treated and non-treated with α-GalCer (Fig. 3C). The ratio of F4/80- and TLR4-positive cells tended to be higher in the α-GalCer-treated mice than in the non-treated mice, but there was no significant difference between the wild-type and IDO-KO mice (Fig. 3D).

Effect of an NO inhibitor on LPS-induced IDO activity in peritoneal cells

Peritoneal cells from α-GalCer-treated wild-type mice (at a rate of 1×10^6 cells/well) were cultured with LPS (100 ng/mL) and L-NAME (4 mM) for 24 h. LPS-induced NO production by the peritoneal cells from α-GalCer-treated wild-type mice was significantly decreased by L-NAME, while the LPS-induced IDO activity was significantly increased by L-NAME (Fig. 4).

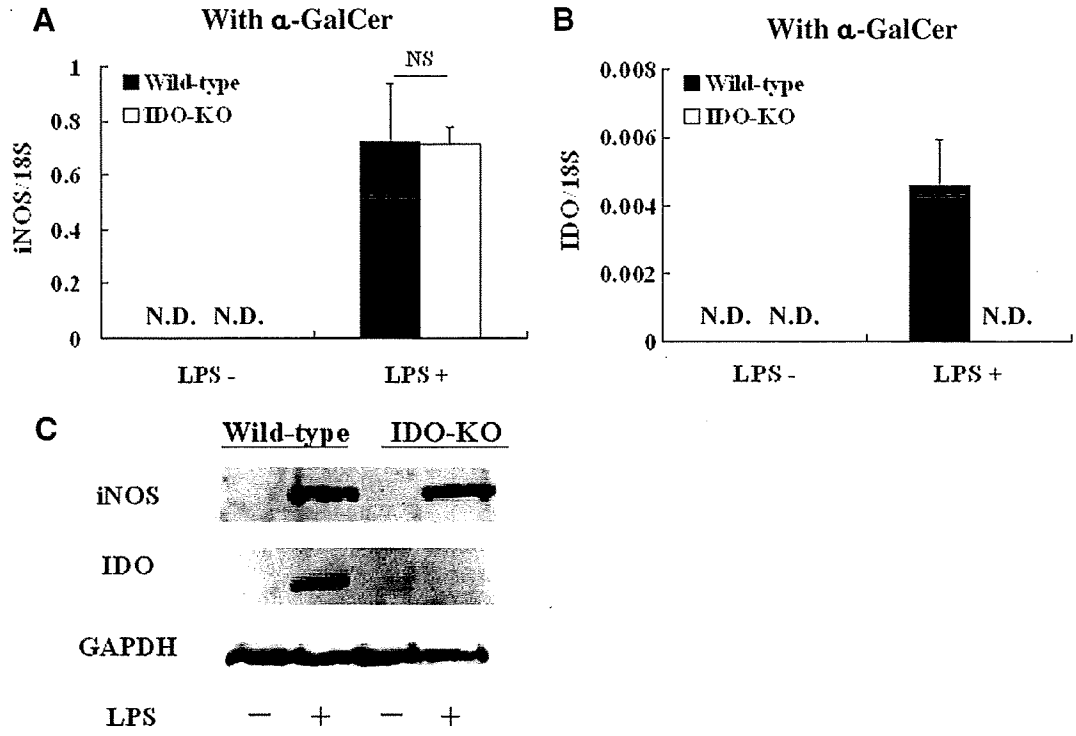

Fig. 2. LPS-induced mRNA and protein expression of iNOS and IDO in peritoneal cells from α-GalCer-treated wild-type and IDO-KO mice. The expression of iNOS and IDO mRNA in peritoneal cells from α-GalCer-treated mice stimulated with LPS (10 ng/mL) for 12 h was analyzed by real-time PCR and was determined on the basis of 18S rRNA expression (A, B). The data are represented as means ± SD of the results of three samples from each group. The expression of the iNOS and IDO proteins in peritoneal cells from α-GalCer-treated mice stimulated with LPS (10 ng/mL) for 24 h was examined by Western blot analysis and was based on the expression of the GAPDH protein (C). These experiments were repeated twice and produced the same results. *$P < 0.05$; N.D.: not detected.

Discussion

In this study, we demonstrated that LPS-induced NO production and IDO activity were enhanced in mouse peritoneal cells obtained after α-GalCer-treatment (Fig. 1A and B). Interestingly, even in such conditions, these two molecules seemed to suppress each other (Figs. 1D and 4B). LPS-induced NO production reached its peak at 12 h after α-GalCer-treatment (Fig. 1A). Previous reports

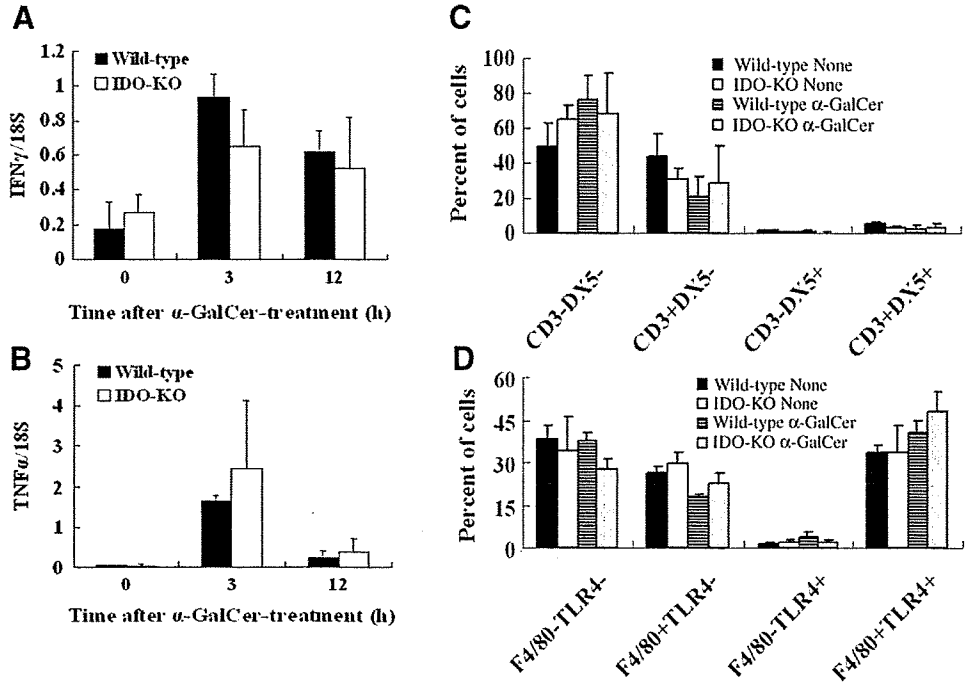

Fig. 3. Effects of α-GalCer on IFN-γ and TNF-α expression and on the phenotype of peritoneal cells from wild-type and IDO-KO mice. Expression of IFN-γ and TNF-α mRNA in peritoneal cells at 0, 3, and 12 h after α-GalCer-treatment was analyzed by real-time PCR and was determined on the basis of 18S rRNA expression (A, B). The percentage of NKT cells (DX5- and CD3-positive cells) and macrophages (F4/80- and TLR4-positive cells) among the peritoneal cells from the non-treated and α-GalCer-treated wild-type and IDO-KO mice was analyzed by flow cytometry (C, D). The data are represented means ± SD of the results of three mice from each group.

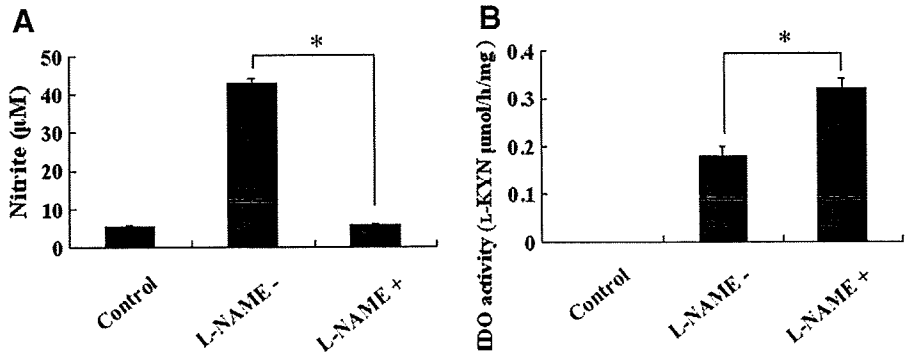

Fig. 4. Effect of an NO inhibitor on IDO activity in peritoneal cells. Peritoneal cells from α-GalCer-treated wild-type mice were cultured at a rate of 1×10^6 cells/well with LPS (100 ng/mL) and L-NAME (4 mM) for 24 h. Cells not treated with LPS were used as the control. The concentration of nitrite in the culture medium was determined (A), and the IDO activity of the cell lysate was determined (B). The data are represented as means ± SD of the results of three samples from each group. $^*P < 0.05$.

indicated that IFN-γ is a very important promoter of iNOS activity and that its production is high at 4–12 h after α-GalCer-treatment [9,21,22], so our results agree well with those of these previous studies. Furthermore, a minute amount of LPS may be adequate to cause inflammatory response in the presence of activated NKT cells, because LPS-induced NO production by peritoneal cells from α-GalCer-treated mice was almost the same at all LPS concentrations (Fig. 1D).

Previous reports suggested that NO interacts with IDO, and that IDO activity is inhibited by an NO donor or a peroxynitrite donor [17,18]. The nitration of the IDO protein inhibits IDO activity, and NO and peroxynitrite inhibit IDO activity in a concentration-dependent manner. It was shown that spermine NONOate and S-nitrosoglutathione markedly inhibit IDO activity at a concentration of over 25 μM. IDO activity was recovered by ceasing of the NO exposure, indicating that the inhibition of IDO activity was reversible. Since IDO mRNA and protein expression showed no changed in the presence of an NO donor, it can be inferred that NO post-translationally regulates IDO activity [18]. Our previous study demonstrated the presence of three nitrated peptides in the peroxynitrite-treated recombinant IDO digests and established the nitration of Tyrosine $(Tyr)^{15}$, Tyr^{345}, and Tyr^{353} residues by two-dimensional liquid chromatography/tandem mass spectrometry [17]. These studies consequently suggest that the nitration of tyrosine residues in the IDO protein by NO and peroxynitrite inhibits IDO activity. In this study, we examined the difference in LPS-induced NO production by peritoneal cells between wild-type and IDO-KO mice. LPS-induced NO production was much higher in the peritoneal cells from α-GalCer-treated IDO-KO mice than in those from α-GalCer-treated wild-type mice (Fig. 1D). However, there was no significant difference in the expression of iNOS mRNA and protein between the wild-type and IDO-KO mice (Fig. 2). Moreover, there was no significant difference in the phenotype (CD3- and DX5-positive cell ratio or F4/80- and TLR4-positive cell ratio) of the peritoneal cells between the wild-type and IDO-KO mice treated or not treated with α-GalCer (Fig. 3C and D). These results show that iNOS was post-translationally regulated by the increased IDO activity. Since the IDO activity was enhanced by an NO inhibitor (Fig. 4), NO may be consumed during IDO inhibition, because of which its production is decreased in wild-type mice (Fig. 1D).

IDO is strongly induced by inflammatory cytokines particularly in macrophages and dendritic cells. Subsequent tryptophan deprivation inhibits T-cell proliferation and suppresses cell-mediated immunity [13,23]. Enhanced IDO activity also induces apoptosis of T cells and differentiation of naïve CD4-positive T cells into Treg cells [24], resulting in the attenuation of an extreme inflammatory response [25–27]. Thus, IDO is thought to play an important role in suppressing severe inflammation. It is suggested that inhibition of IDO activity by excess NO results in exacerbation of inflammation. A strong immune response in severe sepsis is thought to be critical in view of mortality, we previously reported that endotoxic shock is rapidly lethal in the presence of NKT cells activated by α-GalCer [28]. Because NKT cells are strongly activated by acute and chronic viral infections [29], secondary infection by bacteria under such conditions is expected to produce an extremely grave reaction. In the model of endotoxic shock sensitized by α-GalCer, it was confirmed that marked inflammation due to an extreme immune response is histologically observed in the lung and liver, and where iNOS is strongly expressed [9,30]. Our results suggest that a large amount of NO inhibits IDO, which has immunosuppressive function, resulting in further promotion of inflammation in severe endotoxic shock. It is therefore important to regulate IDO in such conditions.

In conclusion, we first reported the effect of Vα14 NKT cell activation on LPS-induced NO production and IDO activity by peritoneal cells from wild-type and IDO-KO mice. These findings may help elucidate the immune mechanism in intra-abdominal bacterial infection.

References

[1] M. Kronenberg, Toward an understanding of NKT cell biology: progress and paradoxes, Annu. Rev. Immunol. 23 (2005) 877–900.
[2] M. Taniguchi, M. Harada, S. Kojo, T. Nakayama, H. Wakao, The regulatory role of Valpha14 NKT cells in innate and acquired immune response, Annu. Rev. Immunol. 21 (2003) 483–513.
[3] R.B. Lorsbach, W.J. Murphy, C.J. Lowenstein, S.H. Snyder, S.W. Russell, Expression of the nitric oxide synthase gene in mouse macrophages activated for tumor cell killing. Molecular basis for the synergy between interferon-gamma and lipopolysaccharide, J. Biol. Chem. 268 (1993) 1908–1913.
[4] S. Ohya, Y. Tanabe, M. Makino, T. Nomura, H. Xiong, M. Arakawa, M. Mitsuyama, The contributions of reactive oxygen intermediates and reactive nitrogen intermediates to listericidal mechanisms differ in macrophages activated pre- and postinfection, Infect. Immun. 66 (1998) 4043–4049.
[5] G. Sass, K. Koerber, R. Bang, H. Guehring, G. Tiegs, Inducible nitric oxide synthase is critical for immune-mediated liver injury in mice, J. Clin. Invest. 107 (2001) 439–447.
[6] S.E. McKim, E. Gabele, F. Isayama, J.C. Lambert, L.M. Tucker, M.D. Wheeler, H.D. Connor, R.P. Mason, M.A. Doll, D.W. Hein, G.E. Arteel, Inducible nitric oxide synthase is required in alcohol-induced liver injury: studies with knockout mice, Gastroenterology 125 (2003) 1834–1844.
[7] H.M. Razavi, L. Wang, S. Weicker, G.J. Quinlan, S. Mumby, D.G. McCormack, S. Mehta, Pulmonary oxidant stress in murine sepsis is due to inflammatory cell nitric oxide, Crit. Care Med. 33 (2005) 1333–1339.
[8] P.L. Beck, Y. Li, J. Wong, C.W. Chen, C.M. Keenan, K.A. Sharkey, D.M. McCafferty, Inducible nitric oxide synthase from bone marrow-derived cells plays a critical role in regulating colonic inflammation, Gastroenterology 132 (2007) 1778–1790.
[9] H. Ohtaki, H. Ito, K. Ando, T. Ishikawa, K. Saito, M. Imawari, T. Yokochi, H. Moriwaki, M. Seishima, Valpha14 NKT cells activated by alpha-galactosylceramide augment lipopolysaccharide-induced nitric oxide production in mouse intra-hepatic lymphocytes, Biochem. Biophys. Res. Commun. 378 (2009) 579–583.

[10] H. Ito, N. Koide, A. Morikawa, F. Hassan, S. Islam, G. Tumurkhuu, I. Mori, T. Yoshida, S. Kakumu, H. Moriwaki, T. Yokochi, Augmentation of lipopolysaccharide-induced nitric oxide production by alpha-galactosylceramide in mouse peritoneal cells, J. Endotoxin Res. 11 (2005) 213–219.
[11] T.W. Stone, L.G. Darlington, Endogenous kynurenines as targets for drug discovery and development, Nat. Rev. Drug Discov. 1 (2002) 609–620.
[12] U. Grohmann, F. Fallarino, P. Puccetti, Tolerance, DCs and tryptophan: much ado about IDO, Trends Immunol. 24 (2003) 242–248.
[13] A.L. Mellor, D.H. Munn, IDO expression by dendritic cells: tolerance and tryptophan catabolism, Nat. Rev. Immunol. 4 (2004) 762–774.
[14] F. Fallarino, U. Grohmann, K.W. Hwang, C. Orabona, C. Vacca, R. Bianchi, M.L. Belladonna, M.C. Fioretti, M.L. Alegre, P. Puccetti, Modulation of tryptophan catabolism by regulatory T cells, Nat. Immunol. 4 (2003) 1206–1212.
[15] U. Grohmann, C. Volpi, F. Fallarino, S. Bozza, R. Bianchi, C. Vacca, C. Orabona, M.L. Belladonna, E. Ayroldi, G. Nocentini, L. Boon, F. Bistoni, M.C. Fioretti, L. Romani, C. Riccardi, P. Puccetti, Reverse signaling through GITR ligand enables dexamethasone to activate IDO in allergy, Nat. Med. 13 (2007) 579–586.
[16] D.H. Munn, M.D. Sharma, J.R. Lee, K.G. Jhaver, T.S. Johnson, D.B. Keskin, B. Marshall, P. Chandler, S.J. Antonia, R. Burgess, C.L. Slingluff Jr., A.L. Mellor, Potential regulatory function of human dendritic cells expressing indoleamine 2,3-dioxygenase, Science 297 (2002) 1867–1870.
[17] H. Fujigaki, K. Saito, F. Lin, S. Fujigaki, K. Takahashi, B.M. Martin, C.Y. Chen, J. Masuda, J. Kowalak, O. Takikawa, M. Seishima, S.P. Markey, Nitration and inactivation of IDO by peroxynitrite, J. Immunol. 176 (2006) 372–379.
[18] S.R. Thomas, A.C. Terentis, H. Cai, O. Takikawa, A. Levina, P.A. Lay, M. Freewan, R. Stocker, Post-translational regulation of human indoleamine 2,3-dioxygenase activity by nitric oxide, J. Biol. Chem. 282 (2007) 23778–23787.
[19] L.C. Green, D.A. Wagner, J. Glogowski, P.L. Skipper, J.S. Wishnok, S.R. Tannenbaum, Analysis of nitrate, nitrite, and [15N]nitrate in biological fluids, Anal. Biochem. 126 (1982) 131–138.
[20] S. Fujigaki, K. Saito, K. Sekikawa, S. Tone, O. Takikawa, H. Fujii, H. Wada, A. Noma, M. Seishima, Lipopolysaccharide induction of indoleamine 2,3-dioxygenase is mediated dominantly by an IFN-gamma-independent mechanism, Eur. J. Immunol. 31 (2001) 2313–2318.
[21] H. Kitamura, K. Iwakabe, T. Yahata, S. Nishimura, A. Ohta, Y. Ohmi, M. Sato, K. Takeda, K. Okumura, L. Van Kaer, T. Kawano, M. Taniguchi, T. Nishimura, The natural killer T (NKT) cell ligand alpha-galactosylceramide demonstrates its immunopotentiating effect by inducing interleukin (IL)-12 production by dendritic cells and IL-12 receptor expression on NKT cells, J. Exp. Med. 189 (1999) 1121–1128.
[22] H. Kitamura, A. Ohta, M. Sekimoto, M. Sato, K. Iwakabe, M. Nakui, T. Yahata, H. Meng, T. Koda, S. Nishimura, T. Kawano, M. Taniguchi, T. Nishimura, Alpha-galactosylceramide induces early B-cell activation through IL-4 production by NKT cells, Cell. Immunol. 199 (2000) 37–42.
[23] D.H. Munn, M. Zhou, J.T. Attwood, I. Bondarev, S.J. Conway, B. Marshall, C. Brown, A.L. Mellor, Prevention of allogeneic fetal rejection by tryptophan catabolism, Science 281 (1998) 1191–1193.
[24] F. Fallarino, U. Grohmann, C. Vacca, R. Bianchi, C. Orabona, A. Spreca, M.C. Fioretti, P. Puccetti, T cell apoptosis by tryptophan catabolism, Cell Death Differ. 9 (2002) 1069–1077.
[25] L. Romani, F. Fallarino, A. De Luca, C. Montagnoli, C. D'Angelo, T. Zelante, C. Vacca, F. Bistoni, M.C. Fioretti, U. Grohmann, B.H. Segal, P. Puccetti, Defective tryptophan catabolism underlies inflammation in mouse chronic granulomatous disease, Nature 451 (2008) 211–215.
[26] L. Romani, T. Zelante, A. De Luca, F. Fallarino, P. Puccetti, IL-17 and therapeutic kynurenines in pathogenic inflammation to fungi, J. Immunol. 180 (2008) 5157–5162.
[27] L. Romani, P. Puccetti, Protective tolerance to fungi: the role of IL-10 and tryptophan catabolism, Trends Microbiol. 14 (2006) 183–189.
[28] H. Ito, N. Koide, F. Hassan, S. Islam, G. Tumurkhuu, I. Mori, T. Yoshida, S. Kakumu, H. Moriwaki, T. Yokochi, Lethal endotoxic shock using alpha-galactosylceramide sensitization as a new experimental model of septic shock, Lab. Invest. 86 (2006) 254–261.
[29] C.A. Biron, L. Brossay, NK cells and NKT cells in innate defense against viral infections, Curr. Opin. Immunol. 13 (2001) 458–464.
[30] G. Tumurkhuu, N. Koide, J. Dagvadorj, A. Morikawa, F. Hassan, S. Islam, Y. Naiki, I. Mori, T. Yoshida, T. Yokochi, The mechanism of development of acute lung injury in lethal endotoxic shock using alpha-galactosylceramide sensitization, Clin. Exp. Immunol. 152 (2008) 182–191.

Biochemical and Biophysical Research Communications 378 (2009) 579–583

Contents lists available at ScienceDirect

Biochemical and Biophysical Research Communications

journal homepage: www.elsevier.com/locate/ybbrc

Vα14 NKT cells activated by alpha-galactosylceramide augment lipopolysaccharide-induced nitric oxide production in mouse intra-hepatic lymphocytes

Hirofumi Ohtaki [a], Hiroyasu Ito [a,*], Kazuki Ando [a], Tetsuya Ishikawa [c], Kuniaki Saito [d], Michio Imawari [e], Takashi Yokochi [f], Hisataka Moriwaki [b], Mitsuru Seishima [a]

[a] Department of Informative Clinical Medicine, Gifu University Graduate School of Medicine, 1-1 Yanagido, Gifu 501-1194, Japan
[b] First Department of Internal Medicine, Gifu University Graduate School of Medicine, 1-1 Yanagido, Gifu 501-1194, Japan
[c] Cancer Immunotherapy Center, Nagoya Kyoritsu Hospital, 1-195 Hoge, Nakagawa, Nagoya, Aichi 454-0933, Japan
[d] Human Health Sciences, Graduate School of Medicine and Faculty of Medicine, Kyoto University, 53 Kawahara-cho, Shogoin, Sakyo, Kyoto 606-8507, Japan
[e] Second Department of Internal Medicine, Showa University School of Medicine, 1-5-8 Hatanodai, Shinagawa-ku, Tokyo 142-8666, Japan
[f] Department of Microbiology and Immunology, Aichi Medical University, Nagakute, Aichi 480-1195, Japan

ARTICLE INFO

Article history:
Received 10 November 2008
Available online 3 December 2008

Keywords:
Vα14 NKT cell
α-Galactosylceramide
Lipopolysaccharide
Nitric oxide
Intra-hepatic lymphocytes

ABSTRACT

Vα14 natural killer T (Vα14 NKT) cells activated by α-galactosylceramide (α-GalCer) secrete a large amount of Th1 and Th2 cytokines. IFN-γ plays a crucial role in the inflammation response, and is also known as an activator of nitric oxide (NO) production. We previously reported that lipopolysaccharide (LPS)-induced NO production is augmented by α-GalCer in mouse peritoneal cells. Since the liver is susceptible to LPS stimulation via the portal vein, we examined the effect of α-GalCer on LPS-induced NO production in murine intra-hepatic lymphocytes (IHLs). Although IHLs augmented LPS-induced NO production by α-GalCer administration, such an augmentation was not observed in non-treated mice. Furthermore, α-GalCer did not augment LPS-induced NO production in IHLs from IFN-γ knockout mice. In flow cytometry analysis of IHLs from α-GalCer-treated mice, the ratio and number of F4/80- and TLR4-positive cells rose as compared with non-treated mice. The liver injury may be induced by LPS and NO under the condition where Vα14 NKT cells were activated.

α-Galactosylceramide (α-GalCer), a glycolipid antigen, specifically activates Vα14 natural killer T (NKT) cells via a CD1d-restricted mechanism. Vα14 NKT cells are a lymphoid lineage characterized by expression of invariant T-cell receptor (TCR) encoded by Vα14-Jα18 gene segments. These cells play a regulatory role in the immunological response under various pathological conditions, including tumor formation, autoimmune diseases, allergy, and infection, by rapidly secreting a large amount of Th1 and Th2 cytokines [1–3]. Additionally, IFN-γ, representative of Th1 cytokines, has been known to elevate nitric oxide (NO) production [4,5].

NO exhibits a wide range of important functions *in vivo*, acting as a relaxing factor mediating vasodilatation, a neuronal messenger molecule, a major regulatory molecule and a principal cytotoxic mediator of the immune system [6–8]. The signal (messenger) molecule NO is synthesized by constitutively expressed NO synthase (cNOS) for short periods of time. The killer (cytotoxic) molecule NO is synthesized by an inducible isoform of NOS (iNOS) that, once expressed, produces NO for long periods of time. It appears paradoxical that NO can both act as a physiological intercellular messenger and display cytotoxic activity *in vivo* [8]. Already, a number of studies have examined the relationship between NO production and tissue injury [9–13]. It was previously reported that NO plays an important role in alcohol-induced liver injury [14], hemorrhagic shock [15], concanavalin A-induced liver injury [16–18], liver damage after GalN/LPS treatment [10], and mycobacterial liver injury [19].

Our previous study reported augmentation of LPS-induced NO production by α-GalCer in mouse peritoneal cells through the release of IFN-γ from Vα14 NKT cells [20]. We thus focused on the liver, which is easily subjected to LPS stimulation via the portal vein and recruits many NKT cells. If α-GalCer augments LPS-induced NO production in intra-hepatic lymphocytes (IHLs), it may give us a clue to understand the association between NO and liver injury under conditions of activated NKT cells. Therefore, the aim of our study was to investigate the effect of α-GalCer on LPS-induced NO production in murine IHLs.

* Corresponding author. Fax: +81 58 230 6431.
E-mail address: hito@gifu-u.ac.jp (H. Ito).

0006-291X/$ - see front matter © 2008 Elsevier Inc. All rights reserved.
doi:10.1016/j.bbrc.2008.11.075

Materials and methods

Reagents. Synthesized α-GalCer was provided by Kirin Brewery Company (Gunma, Japan). LPS from *Escherichia coli* O55:B5 was purchased from Sigma Chemical Co. (St. Louis, MO, USA).

Mice. C57BL/6 and BALB/c mice at approximately 10 weeks of age were obtained from Japan SLC (Hamamatsu, Japan). IFN-γ knockout (−/−) mice were obtained from Jackson Laboratory (Bar Harbor, ME, USA). Jα18 −/− mice as Vα14 NKT cell-deficient mice were kindly provided by T. Nakayama, Chiba University and M. Taniguchi, RIKEN Research Centre. All procedures were conducted in accordance with the National Institutes of Health Guide for the Care and Use of Laboratory Animals, and with the guidelines for care and use of animals established by the Animal Care and Use Committee of Gifu University.

Cell preparation and culture. The mice were sacrificed after intravenous administration of α-GalCer (1 μg/mouse). Liver was perfused with heparinized sterile saline to remove peripheral blood cells, and liver homogenate was passed through stainless steel mesh. IHLs were obtained by the centrifugation of liver homogenate with Ficoll–Hypaque. IHLs were suspended in RPMI 1640 medium containing 10% heat-inactivated fetal calf serum (GIBCO-BRL, Gaithersburg, MD, USA) and 1×10^5 cells/200 μL were seeded on a 96-well microplate, after which LPS was added. After 24 h at 37 °C under 5% CO_2, culture supernatants and IHLs were collected for NO and iNOS mRNA determinations.

Nitrite determination. The nitrite accumulated in the culture medium was measured as an indicator of NO production based on the Griess reaction [21]. The culture supernatant (100 μL) was mixed with 100 μL of Griess reagent, incubated at room temperature for 10 min, and then the absorbance was measured at 570 nm using a microplate reader.

Real-time PCR. Real-time PCR (RT-PCR) was used to quantify the level of iNOS mRNA. Measurements of iNOS mRNA were made in IHL-stimulated by LPS for 24 h with or without α-GalCer. Total RNA was isolated using an Rneasy mini kit (Qiagen GmbH, Hilden, Germany) and modified to cDNA using the Omniscript reverse transcriptase kit (Qiagen). The purified cDNA was used as a template for RT-PCR using predesigned primer/probe sets for the iNOS gene (Assays On Demand; Applied Biosystems, Foster City, CA, USA) and 2× Taqman Universal PCR Master Mix (Applied Biosystems) according to the manufacturer's recommendations. Predesigned primer/probe sets for 18 S were used as an internal control in each reaction well (Applied Biosystems). RT-PCR was carried out using a Light Cycler Rapid Thermal Cycler System (Roche Diagnostic Systems, Indianapolis, USA).

Flow cytometry analysis. Flow cytometry was used to evaluate TLR4 and F4/80 expression of IHLs with or without α-GalCer administration. IHLs were obtained from mice 0, 6 and 12 h after α-GalCer-administration. Following reaction with anti-CD16/CD32 antibody to suppress nonspecific binding, IHLs were stained with fluorescein-isothiocyanate (FITC)-conjugated anti-F4/80 antibody and phycoerythrin (PE)-conjugated anti-TLR4 antibody. The phenotypic characterization of IHLs was carried out using FACScan (Becton-Dickinson, San Jose, CA, USA).

Isolation of CD11b-*positive cells.* IHLs from mice were separated into CD11b-positive and negative cells using anti-CD11b-conjugated magnetic beads (Miltenyi Biotec GmbH, Bergisch Gladbach, Germany). The magnetically labeled cells were purified using VarioMACS system (Miltenyi Biotec GmbH).

Statistical analysis. In each experiment, the results were expressed as mean ± SD. Statistical significance of the difference in mean values was determined by Student's *t*-test, and *p* values of less than 0.05 were considered to be significant.

Results

Effect of α-GalCer on LPS-induced NO production in IHLs

IHLs from non-treated and α-GalCer-treated wild-type mice were cultured at $1x10^5$ cells/well with LPS for 24 h. The concentration of nitrite was determined in culture supernatant. IHLs from the mice at 6 h after α-GalCer treatment produced a little amount of NO in the presence of LPS (0.1 μg/mL), and IHLs from the mice at 12 h after treatment produced a large amount of LPS-induced NO. On the other hand, IHLs from the mice at 0 and 48 h after treatment scarcely produced LPS-induced NO (Fig. 1A). Therefore, IHLs from the mice at 12 h after α-GalCer-treatment were used for the following experiments unless otherwise stated. IHLs from non-treated mice did not produce NO in the presence of high concentrations of LPS (1 and 10 μg/mL) (Fig. 1B). On the other hand, NO production was significantly augmented in IHLs from mice treated with α-GalCer in the presence of low concentrations of LPS (Fig. 1C).

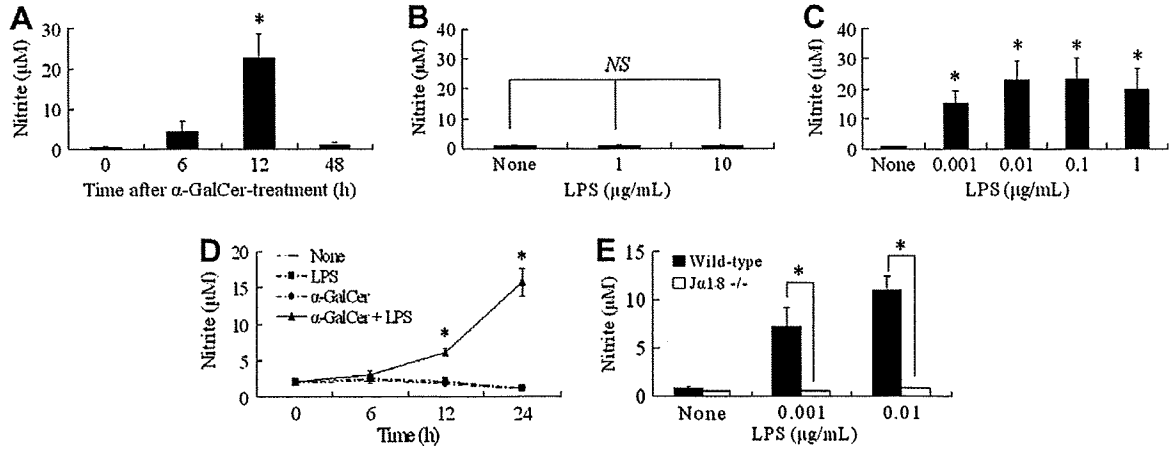

Fig. 1. Effect of α-GalCer on LPS-induced NO production in IHLs. IHLs from the mice at 0, 6, 12 and 48 h after α-GalCer-treatment were cultured at 1×10^5 cells/well with LPS (0.1 μg/mL) (A). In experiment of LPS concentration dependence, IHLs were cultured at 1×10^5 cells/well with LPS. LPS concentration used was 1, 10 μg/mL in non-treated-IHLs (B), and 0.001, 0.01, 0.1, 1 μg/mL in α-GalCer-treated-IHLs (C). The concentration of nitrite in the supernatant was determined 24 h after LPS stimulation. In time course of NO production, LPS concentration used was 10 μg/mL in non-treated-IHLs, and 0.1 μg/mL in α-GalCer-treated-IHLs. The concentration of nitrite in the supernatant was determined 6, 12, and 24 h after LPS stimulation (D). IHLs from α-GalCer-treated wild-type and Jα-281 −/− mice were cultured at 1×10^5 cells/well with LPS (0.001 and 0.01 μg/mL). The concentration of nitrite in the supernatant was determined 24 h after LPS stimulation (E). The data represented are means ± SD from 3 mice of each group. *NS*, not significant; $^*p < 0.05$ vs. 0 h or none.

In time course of LPS-induced NO production, IHLs (1×10^5 cells/well) from non-treated and α-GalCer-treated wild-type mice were stimulated with LPS (non-treated mice:10 μg/ml, α-GalCer-treated mice:0.1 μg/ml) for 6, 12, and 24 h. LPS-induced NO production in IHLs from α-GalCer-treated mice increased after 12 h and at 24 h reached approximately twice that at 12 h. On the other hand, the enhancement of NO production was not observed in IHLs from non-treated mice through 24 h (Fig. 1D).

To examine direct effect by α-GalCer, IHLs from α-GalCer-treated wild-type and Jα18 −/− mice were cultured at 1×10^5 cells/well with LPS (0.001 and 0.01 μg/mL) for 24 h. Although IHLs from wild-type mice augmented LPS-induced NO production, such an augmentation was not observed in Jα18 −/− mice (Fig. 1E).

Comparison of NO production and iNOS mRNA level between wild-type and IFN-γ −/− mice with α-GalCer administration

IHLs from the wild-type and IFN-γ −/− mice at 12 h after α-GalCer-treatment were cultured at 1×10^5 cells/well with LPS for 24 h. Culture supernatant was used for the determination of nitrite. NO production in IHLs from α-GalCer-treated wild- type mice significantly increased with LPS stimulation. On the other hand, α-GalCer did not augment LPS-induced NO production in IHLs from IFN-γ −/− mice (Fig. 2A).

The expression of iNOS mRNA in IHLs stimulated with LPS was examined with real-time RT-PCR and was determined based on 18S mRNA. IHLs from wild-type mice and IFN-γ −/− mice with or without α-GalCer administration were cultured at 1×10^5 cells/well with LPS for 24 h. The expression of iNOS mRNA in IHLs from α-GalCer-treated wild-type mice was significantly enhanced with LPS stimulation, but that in IHLs from α-GalCer-treated IFN-γ −/− mice was not (Fig. 2B).

Identification of NO producing cells

CD11b-positive and CD11b-negative cells in IHLs from the wild-type mice at 0 and 12 h after α-GalCer-treatment were isolated by magnetic cell sorting. Each cell type was cultured at 1×10^5 cells/200 μL with LPS (1 μg/mL) for 24 h. Culture supernatant was subjected for determination of the nitrite concentration. LPS-induced NO production was significantly augmented in CD11b-positive cells from α-GalCer-treated mice. On the other hand, in CD11b-negative cells from α-GalCer-treated mice and each cells from non-treated mice, such an enhancement of LPS-induced NO production was not observed (Fig. 3).

Effect of α-GalCer on cell ratio and cell number of F4/80 and TLR4 double-positive cell in IHLs

Next, by reason that CD11b-positive cells significantly produced LPS-induced NO, we examined the ratio and number of F4/80- and

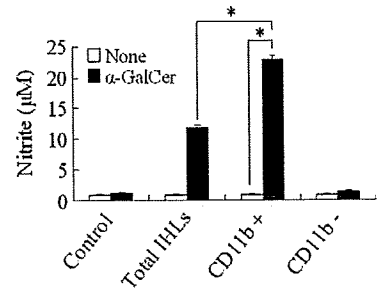

Fig. 3. Identification of NO producing cells. CD11b-positive cells were isolated from IHLs of non- and α-GalCer-treated wild-type mice by magnetic cell sorting. Each cells (total IHLs, CD11b-positive IHLs and CD11b-negative IHLs) was cultured at 1×10^5 cells/200 μL with LPS (1 μg/mL) for 24 h. The concentration of nitrite was determined in culture supernatant. The data represented are means ± SD in triplicate cultures. Control is LPS-untreated total IHLs. *$p < 0.05$.

TLR4-positive cells which have recognition mechanism to LPS in IHLs from non-treated and α-GalCer-treated wild-type mice. The mice were sacrificed at 0 (non-treatment), 6, 12 and 48 h after α-GalCer-treatment and IHLs were obtained. After IHLs were reacted with anti-CD16/CD32 antibody, they were stained with FITC-conjugated anti-F4/80 antibody and PE-conjugated anti-TLR4 antibody. Although IHLs from the mice at 12 h after treatment contained 14.6 ± 2.3% of F4/80 and TLR4 double-positive cells based on non-staining controls, those from the mice at 0, 6 and 48 h after treatment contained 6.6 ± 0.1%, 6.3 ± 0.8% and 7.9 ± 2.5% (Fig. 4A and B). Thus, IHLs from the mice at 12 h after treatment contained a higher proportion of F4/80 and TLR4 double-positive cells as compared with those from the mice at 0, 6 and 48 h after treatment. Also, F4/80 and TLR4 double-positive cell number from the mice at 12 h after treatment had increased as compared with those from the mice at 0, 6 and 48 h after treatment (Fig 4C).

Discussion

In the present study, we demonstrated that activation of Vα14 NKT cells by α-GalCer augments LPS-induced NO production in murine IHLs. Since such enhancement was not observed in IFN-γ −/− mice, it is suggested that IFN-γ secreted by Vα14 NKT cells activated with α-GalCer contributes to the augmentation of LPS-induced NO production in IHLs.

The liver plays an important role in the development of multiple organ failure (MOF) during sepsis. Whereas the gut is considered to be a main causative organ of MOF, the liver acts as the modulator of it [22]. Pathophysiologically, hypoperfusion of the gut during endotoxemia leads to disruption of the mucosal barrier following subsequent translocation of LPS to the portal vein [23,24]. Therefore, these reports agree that the liver is exposed to

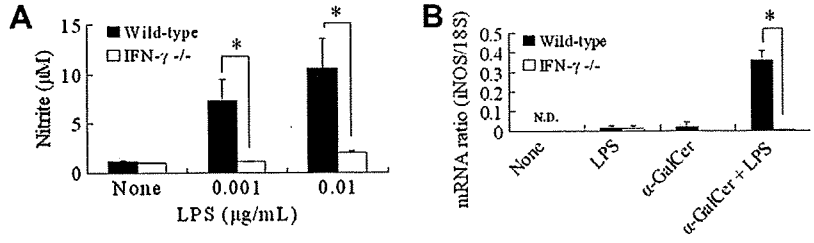

Fig. 2. Comparison of NO production and iNOS mRNA level between wild-type and IFN-γ KO mice with α-GalCer administration. IHLs were cultured at 1×10^5 cells/well with LPS. LPS concentration used was 0.001, 0.01 μg/mL in α-GalCer-treated-IHLs. The concentration of nitrite in the supernatant was determined 24 h after LPS stimulation (A). IHLs (1×10^5 cells/well) were cultured with LPS (α-GalCer treated-IHLs: 0.001 μg/mL, non-treated-IHLs: 10 μg/mL) for 24 h. The expression of iNOS mRNA was analyzed by real-time PCR and was determined based on 18 S mRNA (B). The data represented are means ± SD from 3 mice of each group. *$p < 0.05$.

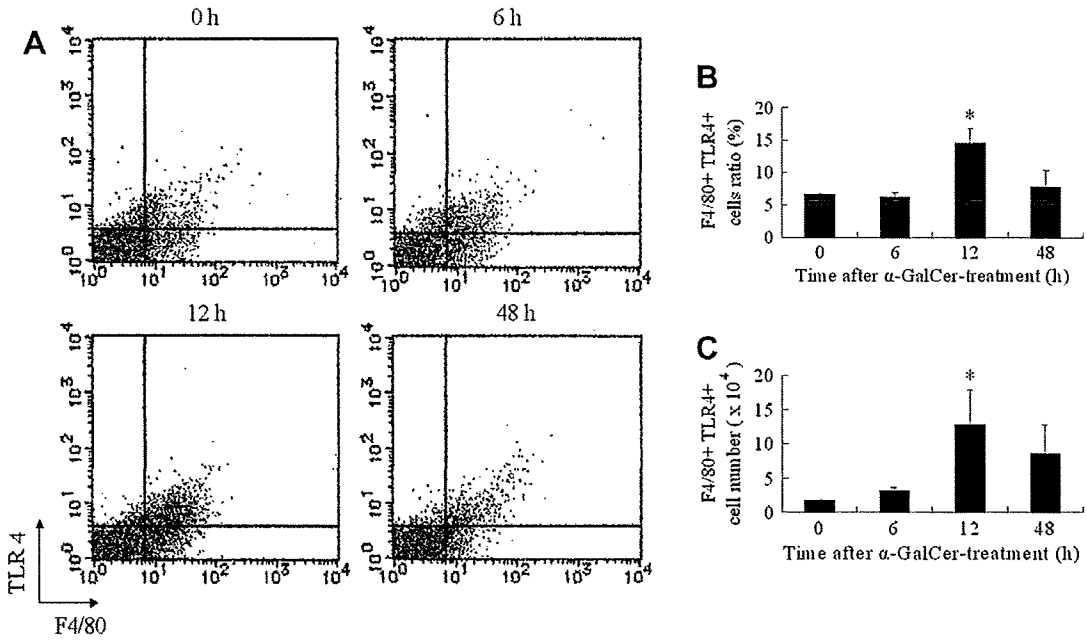

Fig. 4. Effect of α-GalCer on cell ratio and cell number of F4/80 and TLR4 double-positive cell in IHLs. The mice were sacrificed 0, 6, 12, and 48 h after α-GalCer-treatment and IHLs were obtained. After IHLs were reacted with anti-CD16/CD32 antibody, they were stained with anti-F4/80 (FITC, FL-1) and anti-TLR4 (PE, FL-2) antibody (A,B). And, F4/80 and TLR4 double-positive cell number was also measured (C). The data represented are means ± SD from 3 mice of each group. $^{*}p < 0.05$ vs. 0 h.

LPS stimulation and LPS-induced NO is then involved in the liver injury. In fact, several studies have examined the relationship between NO production and liver injury [10,14–18]. In the present study, LPS-induced NO production in IHLs from non-treated mice was not observed even in the presence of a high concentration of LPS (Fig. 1B). Thus, IHLs in their normal state may be not so susceptible to LPS, because sinusoidal cells including Kupffer cells are first exposed to LPS.

As a responsible molecule for NO-induced liver injury, peroxynitrite, a potent oxidant formed from NO and superoxide, has a higher reactivity than NO. Therefore, its toxicity to the liver may be considerably high. Peroxynitrite causes tyrosine nitration resulting in the formation of nitrotyrosine [6]. Actually, nitrotyrosine was detected at the sites of LPS-induced hepatic injury in D-galactosamine-sensitized mice, peroxynitrite appeared to cause hepatic injury [10], indicating that NO production strongly contributes to hepatic injury. Indeed, our results suggest that IHLs from α-GalCer-treated mice augmented LPS-induced NO production; in particular, CD11b-positive cells in IHLs produce LPS-induced NO (Fig. 3). Therefore, these data revealed that CD11b-positive cells were enhanced an ability to produce NO by α-GalCer. Previous reports indicated that IFN-γ production exhibit high value 4–12 h after α-GalCer-treatment [25,26] and our result demonstrated that IHLs from the mice at 12 h after α-GalCer-treatment highly produced NO. As shown in Fig. 1A, IHLs from the mice 0 and 48 h after α-GalCer-treatment did not produce NO. This data suggested that there is the correlation between LPS-induced NO production and IFN-γ production. It is common knowledge that IFN-γ is very important activator of iNOS. Since augmentation of NO production was not observed in Jα18 −/− mice and IFN-γ −/− mice, it was thought that IFN-γ from Vα14 NKT cell activated by α-GalCer is very important in this phenomenon. We also showed that the cell ratio and cell number of F4/80- and TLR4-positive cells which have recognition mechanism to LPS in IHLs rose by α-GalCer-treatment (Fig. 4). Consequently, it is assumed that both enhanced abilities of CD11b-positive cells and increased numbers of it is important in LPS-induced NO production.

The liver is highly susceptible to LPS in Vα14 NKT cell-activated state. It was previously reported that invariant NKT cells respond to the progressive liver damage caused by chronic hepatitis virus infection [27]. Moreover, invariant NKT cells have substantial effector potential, which characterizes the chronic liver damage, and also have the capacity to produce IL-4 and IL-13 besides IFN-γ. It is likely that the stage of liver disease depends on the activity of invariant NKT cells. Virus infection of the liver could potentially directly or indirectly provoke the activation of NKT cells, because NKT cells are abundant in the liver and a high amount of CD1d molecules are seen on hepatocytes [28]. On the other hand, CD1d-deficient mice have an increased susceptibility to encephalomyocarditis virus (EMCV), suggesting a physiological role of the CD1d molecule and/or CD1d-restricted T cells. Recently, Brion et al. examined the role of NKT cells during EMCV infection and found that, at 36 h after infection, the hepatic NKT cell population was dramatically reduced. This finding suggests an early activation of NKT cells, because stimulation of this population results in activation-induced cell death. It is thus considered that acute and chronic viral infections induce the activation of NKT cells. Our results that LPS-induced NO production is augmented by α-GalCer in IHLs raise the possibility that activation of NKT cells is involved in the liver injury via LPS and NO. In particular, chronic liver damage caused by hepatitis virus or autoimmune mechanisms may induce the activation of NKT cells in the liver, and the enhancement of LPS-induced NO production may contribute to liver injury.

In conclusion, we demonstrated that Vα14 NKT cells activated by alpha-galactosylceramide augment lipopolysaccharide-induced NO production in mouse intra-hepatic lymphocytes. We propose that while NKT cells have important roles in many infectious diseases and hepatic immunity, activation of NKT cells may elevate the sensitivity of the liver to NO via LPS.

Acknowledgments

We are grateful to Dr. T. Nakayama and Dr. M. Taniguchi for providing Vα14 NKT-deficient mice. We express our gratitude to

John Cole for reading our draft and giving us suggestions on language and style.

References

[1] M. Kronenberg, Toward an understanding of NKT cell biology: progress and paradoxes, Annu. Rev. Immunol. 23 (2005) 877–900.
[2] M. Kronenberg, L. Gapin, The unconventional lifestyle of NKT cells, Nat. Rev. Immunol. 2 (2002) 557–568.
[3] M. Taniguchi, M. Harada, S. Kojo, T. Nakayama, H. Wakao, The regulatory role of Valpha14 NKT cells in innate and acquired immune response, Annu. Rev. Immunol. 21 (2003) 483–513.
[4] R.B. Lorsbach, W.J. Murphy, C.J. Lowenstein, S.H. Snyder, S.W. Russell, Expression of the nitric oxide synthase gene in mouse macrophages activated for tumor cell killing. Molecular basis for the synergy between interferon-gamma and lipopolysaccharide, J. Biol. Chem. 268 (1993) 1908–1913.
[5] C. Nathan, Nitric oxide as a secretory product of mammalian cells, FASEB J. 6 (1992) 3051–3064.
[6] J.S. B eckman, W.H. K oppenol, Nitric oxide, superoxide, and peroxynitrite: the good, the bad, and ugly, Am. J. Physiol. 271 (1996) C1424–C1437.
[7] S. Dimmeler, A.M. Zeiher, Nitric oxide and apoptosis: another paradigm for the double-edged role of nitric oxide, Nitric Oxide 1 (1997) 275–281.
[8] K.D. Kroncke, K. Fehsel, V. Kolb-Bachofen, Nitric oxide: cytotoxicity versus cytoprotection—how, why, when, and where?, Nitric Oxide 1 (1997) 107–120
[9] S. Milano, F. Arcoleo, P. D'Agostino, E. Cillari, Intraperitoneal injection of tetracyclines protects mice from lethal endotoxemia downregulating inducible nitric oxide synthase in various organs and cytokine and nitrate secretion in blood, Antimicrob. Agents Chemother. 41 (1997) 117–121.
[10] A. Morikawa, Y. Kato, T. Sugiyama, N. Koide, D. Chakravortty, T. Yoshida, T. Yokochi, Role of nitric oxide in lipopolysaccharide-induced hepatic injury in D-galactosamine-sensitized mice as an experimental endotoxic shock model, Infect. Immun. 67 (1999) 1018–1024.
[11] T. Genovese, S. Cuzzocrea, R. Di Paola, M. Failla, E. Mazzon, M.A. Sortino, G. Frasca, E. Gili, N. Crimi, A.P. Caputi, C. Vancheri, Inhibition or knock out of inducible nitric oxide synthase result in resistance to bleomycin-induced lung injury, Respir. Res. 6 (2005) 58.
[12] P.L. Beck, Y. Li, J. Wong, C.W. Chen, C.M. Keenan, K.A. Sharkey, D.M. McCafferty, Inducible nitric oxide synthase from bone marrow-derived cells plays a critical role in regulating colonic inflammation, Gastroenterology 132 (2007) 1778–1790.
[13] H. Lu, B. Zhu, X.D. Xue, Role of neuronal nitric oxide synthase and inducible nitric oxide synthase in intestinal injury in neonatal rats, World J. Gastroenterol. 12 (2006) 4364–4368.
[14] S.E. McKim, E. Gabele, F. Isayama, J.C. Lambert, L.M. Tucker, M.D. Wheeler, H.D. Connor, R.P. Mason, M.A. Doll, D.W. Hein, G.E. Arteel, Inducible nitric oxide synthase is required in alcohol-induced liver injury: studies with knockout mice, Gastroenterology 125 (2003) 1834–1844.
[15] J. Menezes, C. Hierholzer, S.C. Watkins, V. Lyons, A.B. Peitzman, T.R. Billiar, D.J. Tweardy, B.G. Harbrecht, A novel nitric oxide scavenger decreases liver injury and improves survival after hemorrhagic shock, Am. J. Physiol. 277 (1999) G144–G151.
[16] G. Sass, K. Koerber, R. Bang, H. Guehring, G. Tiegs, Inducible nitric oxide synthase is critical for immune-mediated liver injury in mice, J. Clin. Invest. 107 (2001) 439–447.
[17] K. Koerber, G. Sass, A.K. Kiemer, A.M. Vollmar, G. Tiegs, In vivo regulation of inducible no synthase in immune-mediated liver injury in mice, Hepatology 36 (2002) 1061–1069.
[18] A. Mabuchi, T. Nagao, O. Koshio, T. Ishiwata, A. Yano, K. Suzuki, K. Yokomuro, A.M. Wheatley, Role of F4/80Mac-1 adherent non-parenchymal liver cells in concanavalin A-induced hepatic injury in mice, Hepatol. Res. 38 (2008) 1040–1049.
[19] R. Guler, M.L. Olleros, D. Vesin, R. Parapanov, C. Vesin, S. Kantengwa, L. Rubbia-Brandt, N. Mensi, A. Angelillo-Scherrer, E. Martinez-Soria, F. Tacchini-Cottier, I. Garcia, Inhibition of inducible nitric oxide synthase protects against liver injury induced by mycobacterial infection and endotoxins, J. Hepatol. 41 (2004) 773–781.
[20] H. Ito, N. Koide, A. Morikawa, F. Hassan, S. Islam, G. Tumurkhuu, I. Mori, T. Yoshida, S. Kakumu, H. Moriwaki, T. Yokochi, Augmentation of lipopolysaccharide-induced nitric oxide production by alpha-galactosylceramide in mouse peritoneal cells, J. Endotoxin Res. 11 (2005) 213–219.
[21] L.C. Green, D.A. Wagner, J. Glogowski, P.L. Skipper, J.S. Wishnok, S.R. Tannenbaum, Analysis of nitrate, nitrite, and [15N]nitrate in biological fluids, Anal. Biochem. 126 (1982) 131–138.
[22] G.M. Matuschak, J.E. Rinaldo, Organ interactions in the adult respiratory distress syndrome during sepsis, role of the liver in host defense, Chest 94 (1988) 400–406.
[23] P. Baron, L.D. Traber, D.L. Traber, T. Nguyen, M. Hollyoak, J.P. Heggers, D.N. Herndon, Gut failure and translocation following burn and sepsis, J. Surg. Res. 57 (1994) 197–204.
[24] H. Schmidt, A. Secchi, R. Wellmann, A. Bach, H. Bohrer, M.M. Gebhard, E. Martin, Effect of endotoxemia on intestinal villus microcirculation in rats, J. Surg. Res. 61 (1996) 521–526.
[25] H. Kitamura, K. Iwakabe, T. Yahata, S. Nishimura, A. Ohta, Y. Ohmi, M. Sato, K. Takeda, K. Okumura, L. Van Kaer, T. Kawano, M. Taniguchi, T. Nishimura, The natural killer T (NKT) cell ligand alpha-galactosylceramide demonstrates its immunopotentiating effect by inducing interleukin (IL)-12 production by dendritic cells and IL-12 receptor expression on NKT cells, J. Exp. Med. 189 (1999) 1121–1128.
[26] H. Kitamura, A. Ohta, M. Sekimoto, M. Sato, K. Iwakabe, M. Nakui, T. Yahata, H. Meng, T. Koda, S. Nishimura, T. Kawano, M. Taniguchi, T. Nishimura, Alpha-galactosylceramide induces early B-cell activation through IL-4 production by NKT cells, Cell. Immunol. 199 (2000) 37–42.
[27] C. de Lalla, G. Galli, L. Aldrighetti, R. Romeo, M. Mariani, A. Monno, S. Nuti, M. Colombo, F. Callea, S.A. Porcelli, P. Panina-Bordignon, S. Abrignani, G. Casorati, P. Dellabona, Production of profibrotic cytokines by invariant NKT cells characterizes cirrhosis progression in chronic viral hepatitis, J. Immunol. 173 (2004) 1417–1425.
[28] C.A. Biron, L. Brossay, NK cells and NKT cells in innate defense against viral infections, Curr. Opin. Immunol. 13 (2001) 458–464.